DOI 10.1007/s11237-015-9401-2
Theoretical and Experimental Chemistry, Vol. 51, No. 2, May, 2015 (Russian Original Vol. 51, No. 2, March-April, 2015)

PREPARATION, STRUCTURE, AND PROPERTIES OF HYBRID POLYMER COMPOSITES CONTAINING SILVER CLUSTERS AND NANOPARTICLES

A. L. Tolstov

UDC 678.82:661.857:544(14+77)

The major methods for the preparation of silver-containing polymer composite nanosystems and the formation of their hybrid structure are examined. Special attention is focused on a new class of silver-containing hybrid systems, namely, organic–inorganic coordination polymers, obtained by the self-assembly of silver complexes. The effect of intercomponent interaction on the structure and properties of these hybrid composites was examined.

Key words: *hybrid materials, polymers, silver clusters and nanoparticles, structure, properties.*

The creation of new improved materials is an important goal of modern chemistry and materials science. Polymer composites with hybrid structure are among such materials and hold interest since they display a combination of properties characteristic for each of the inorganic and organic components [1-3] and, in some cases, unique properties related to the specific nature of their structure [4]. From a modern viewpoint, hybrid organic–inorganic materials are formed by the combination of components, differing in their chemical nature, on a molecular or nano level through formation of chemical bonds ((non)covalent bonds, hydrogen bonding, and donor–acceptor bonds) or weaker physical bonds (van der Waals and electrostatic interactions) [5]. Special attention is given to the stability of the nanodispersed components due to interaction between the nanophase and various stabilizers [6]. The interest in silver-containing hybrid polymer composite materials, including nanocomposites, which, by their very nature, are *a priori* hybrid systems, is attributed to a set of properties of the matrix itself, which often possesses hybrid structure, properties of silver in ionic and nanodispersed forms, and new properties related to the appearance of hybrid silver–polymer structures [7, 8]. Special interest is presently found in bionanocomposites derived from biopolymers and silver nanoparticles (SN), which display specific physicochemical properties, in particular, electrochemical, photochemical, and catalytic properties highly dependent on the dimensions and polydispersion of the nanophase [9, 10] as well as biological activity due to the ionization of the metal atoms in the presence of H_2O/O_2 and the interaction between the SN surface and functional groups of the various biomolecules [11].

In light of the important role of the polymer matrix in formation of the major structural characteristics and properties of silver-containing hybrid systems, we should classify these materials according to their chemical structure.

Composites with Silver Nanoparticles (SN) Dispersed in a Polymer Matrix with Hybrid Structure. The major distinguishing feature of such materials is the prior synthesis of the hybrid polymer matrix obtained due to the formation of chemical bonds between the organic and inorganic components with subsequent introduction of SN into the system. The synthesis of the SN may be either *in situ* or *ex situ*.

Institute of Macromolecular Chemistry, National Academy of Sciences of Ukraine, Kharkivs'ke Shose, 48, Kyiv 02160, Ukraine. E-mail: tolstov.aleksandr@rambler.ru. Translated from Teoreticheskaya i Éksperimental'naya Khimiya, Vol. 51, No. 2, pp. 67-87, March-April, 2015. Original article submitted January 14, 2015.

Hybrid Systems with an Organic Polymer Matrix. Such nanosystems include traditional composites consisting of an organic polymer matrix with dispersed SN. We should note that such nanosystems may contain another highly-dispersed phase in addition to SN such as silica or carbon fillers as well as globular biomacromolecules, which significantly complicates their structure. Interaction between SN (or another nanodispersed component) and the organic matrix as well as between nanodispersed phases of the nanocomposites affects the final properties.

Silver-Containing Coordination Polymers. Hybrid polymer systems formed upon the self-assembly of a series of silver-containing coordination compounds to give polymer structures featuring metal–metal bonds are a relatively new class of such materials. These bonds permit formation of silver clusters with various degrees of complexity and impart characteristic properties such as luminescence and strong electrical conductance.

In this work, we present the major methods for obtaining silver-containing composite nanosystems, in which formation of the hybrid structure occurs due to reaction between the inorganic and organic components. We examine the chemical and phase structure of these materials as well as the major features holding promise for practical application.

COMPOSITES WITH SN DISPERSED IN A POLYMER MATRIX WITH HYBRID STRUCTURE

Composite polymer systems with SN dispersed in a hybrid polymer matrix are a common type of silver-containing hybrid materials. Among the methods for their preparation, sol–gel synthesis and polymerization methods permitting the efficient formation of a hybrid matrix are most commonly used [12].

The sol–gel method has been used to obtain multilayer aminated PET/TiO_2/chitosan/heparin hybrid composites containing SN by the thermally-induced reduction of Ag^+ ions in a nitrogen atmosphere, which imparts strong bactericidal activity [13]. Coatings were obtained similarly from $Si(OC_2H_5)_4$, SN, and polyvinyl alcohol (PVA) as the reducing agent [14]. Furthermore, the reducing properties of low-molecular-weight [15] and high-molecular-weight hydrides [16, 17] as well as polymers with OH and CO_2H functional groups [18] may be used for the formation of silver-containing hybrid systems. Composites obtained from PVA, $H_2N(CH_2)_3Si(C_2H_5O)_3$, and SN with immobilized *Trichosporon cutaneum R57* cells have enhanced capacity for the adsorption of Mn^{2+} ions [19]. The introduction of amylase enzyme into the surface layer of such systems permits them to catalyze the hydrolysis of starch in a broad pH range [20]. The amino groups in the structure of hybrid materials facilitate the immobilization of protein macromolecules and SN on the composite surface [20, 21].

The reduction of Ag^+ ions in the hybrid matrix obtained by the sol–gel method from $Si(OC_2H_5)_4$, polyhedral oligomeric silsesquioxane (POSS), functionalized by PEG, and the triblock poly(*p*-dioxanone-ε-caprolactone)-PEG-poly(*p*-dioxanone-ε-caprolactone) copolymer gives nanocomposites, in which POSS-$(PEG)_8$ acts as a compatibilizer for inorganic (SiO_2/SN) and the organic (or block copolymer) components [22]. These composites display luminescence with maxima at 318 and 631 nm (λ_{exc} = 250 nm) due to electronic transitions on the SiO_2/SN boundary.

Aflori et al. [23] found that highly stable hybrid systems were obtained by the reduction of Ag^+ ions in a copolymer matrix derived from 3-(trimethoxysilyl)propyl methacrylate (TSM) and $Ti(OCH_3)_4$. The change in structure of the hybrid matrix upon its synthesis from $Zr(OCH_3)_4$ and polytetramethylene glycol (PTMG) leads to deterioration of its stabilizing activity relative to SN and to an increase in the diameter of these particles from 4-6 to 20-80 nm [24]. Despite these features, the nanocomposites obtained are stable in the atmosphere and possess bactericidal and fungicidal properties, while hybrid fibers obtained by the thermally-initiated reduction of Ag^+ ions in the matrix of the copolymer derived from $Si(OC_2H_5)_4$ and TSM may catalyze the reduction of methylene blue (MB) dye [25].

The reactive formation method is extensively used in the formation of hybrid systems. Ultrasonic treatment of a mixture of benzidine, $H_3PMo_{12}O_{40}$, and $AgNO_3$ yielded polybenzidine/$H_3PMo_{12}O_{40}$/SN composites with sensor sensitivity toward $HalO_3^-$ (Hal = Cl, Br, I) equal to $(0.086\text{-}1.66)\cdot10^{-6}$ mol [26]. Aniline (An) was used in analogous procedure to obtain an H_2O_2 sensor with sensitivity ~$0.75\cdot10^{-6}$ mol [27]. The hybrid structure of the composites is also formed upon curing of the copolymer of $Si(OC_2H_5)_4$, 3-(glycidyloxypropyl)trimethoxysilane, and $Ti(OC_2H_5)_4$ in the presence of PEG and $AgNO_3$ [28]. By varying the composition of the hybrid materials, we may alter their optical (refraction index *n* in the range 1.475-1.710) and catalytic properties in the alkynylation of trifluoromethyl ketones and aromatic aldehydes in aqueous media [17, 28].

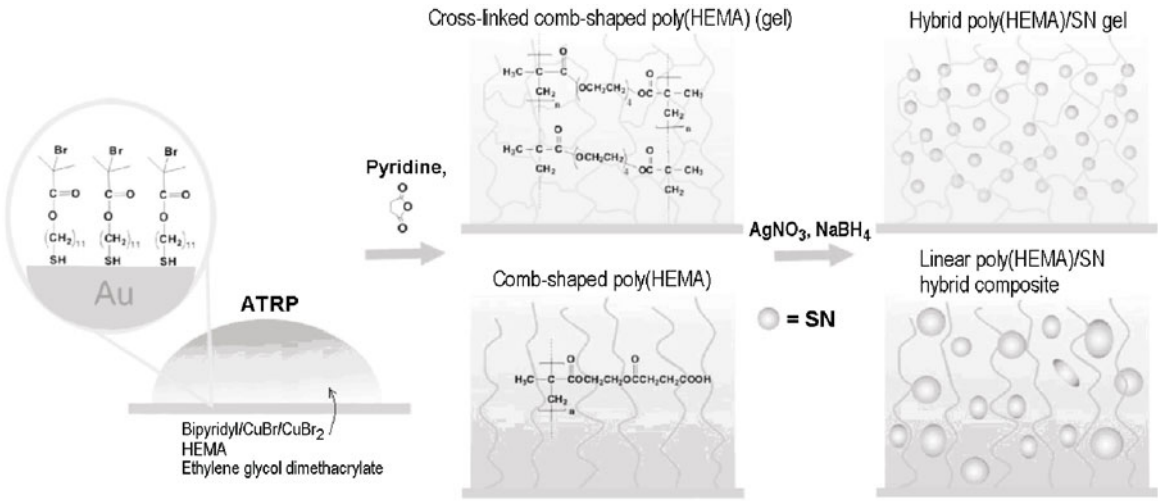

Fig. 1. Scheme for the synthesis of hybrid poly(HEMA)/SN coatings with different matrix structure. Reprinted with permission from Benetti et al. [35]. Copyright © 2010, Wiley VCH Verlag GmbH, KGaA, Weinheim.

The photopolymerization of phenylmaleimide-containing trialkoxysilane (PMTES) and polyurethane acrylate derived from polydimethylsiloxane (PDMS) in the presence of SN with subsequent hydrolysis gave hybrid systems with hydrophobicity subject to controlled variation, thermal stability, and bactericidal activity [29]. Materials with a similar set of properties were obtained by the photopolymerization of a sol obtained from PDMS with terminal triethoxysilyl groups and TSM, alkyl diacrylate, and PDMS-containing polyurethane acrylate [30]. The copolymerization of polyurethane acrylate with TSM sol in the presence of SN gave nanocomposites, whose mechanical properties as well as thermal and chemical stability depend strongly on the content of the inorganic phase [31]. The photoinitiated polymerization of N-vinylpyrrolidone (VP), CH_2=CHSi$(OCH_3)_3$, oligourethane acrylate, and a sol obtained by the hydrolysis of TSM and bis[(4-β-hydroxyethoxy)phenyl]methylphosphine oxide carbamate with terminal Si$(OCH_3)_3$ groups (the sol–gel matrix synthesis is commonly used in the formation of such composites [32]) in the presence of SN gave hybrid systems with improved mechanical and bactericidal properties, enhanced hydrophilicity, and high thermal stability [33]. Composites obtained by the copolymerization of methacrylic acid (MAA), divinylbenzene, and SN modified with TSM using the molecular imprinting method have sensor sensitivity toward 4-mercaptobenzoic acid down to 10^{-15} mol [34].

Controlled polymerization is often used for preparing hybrid materials. Modification of the gold surface with bifunctional initiator ($HS(CH_2)_{11}OC(O)C(CH_3)_2Br$) permits use of the atom transfer radical polymerization method (ATRP) for grafting a layer of the poly(2-hydroxyethyl methacrylate)(poly(HEMA)) hydrogel as an efficient adsorbent of SN and the preparation of hybrid nanosystems with high thermal and electrical conductance and enhanced strength as well as pronounced bactericidal and sensor activity (Fig. 1) [35]. Benetti et al. [35] established that the size of the SN and properties of the system may be altered by varying the extent of cross-linking of poly(HEMA). The grafting of poly(HEMA) onto a glass membrane surface and subsequent immobilization of SN imparts catalytic activity in the reduction of 4-nitrophenol (4NT) [36]. Analogously, composites were obtained using polyelectrolytes with $N(R)_3^+$, CO_2H, and SO_3H groups as the polymer component [37]. The presence of quaternary nitrogen in the structure of the macromolecules enhances the bactericidal activity of the composites, while the zwitter-ionic nature of the polymers imparts resistance to the formation of bacterial biofilms.

Carbon fillers are commonly used as additional inorganic components in the preparation of hybrid systems containing SN [38-41]. Electroactive nanocomposites are formed upon the reduction of the Ag^+ ions in a dispersion of multiwalled carbon nanotubes (MCNT) stabilized by a PEG-oligoimid block copolymer. The SN aggregation and structurized matrices in these nanocomposites facilitate a bridging effect with increasing temperature between the particles of the MCNT-SN hybrid filler and decrease the resistivity R from $2.1 \cdot 10^5$ to $2.0 \cdot 10^{-1}$ Ω·cm [42]. The addition of nanocrystalline TiO_2 into such systems imparts photocatalytic properties [43].

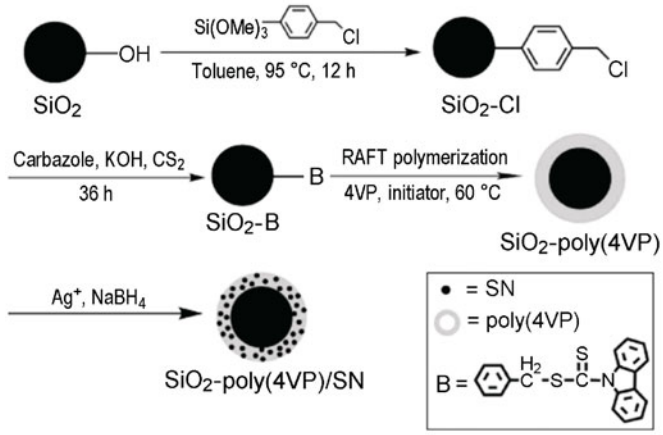

Fig. 2. Scheme for the preparation of hybrid nanoparticles with core–shell structure derived from SiO_2 and poly(4VP). Reprinted with the permission of Liu et al. [52]. Copyright © 2010, American Chemical Society.

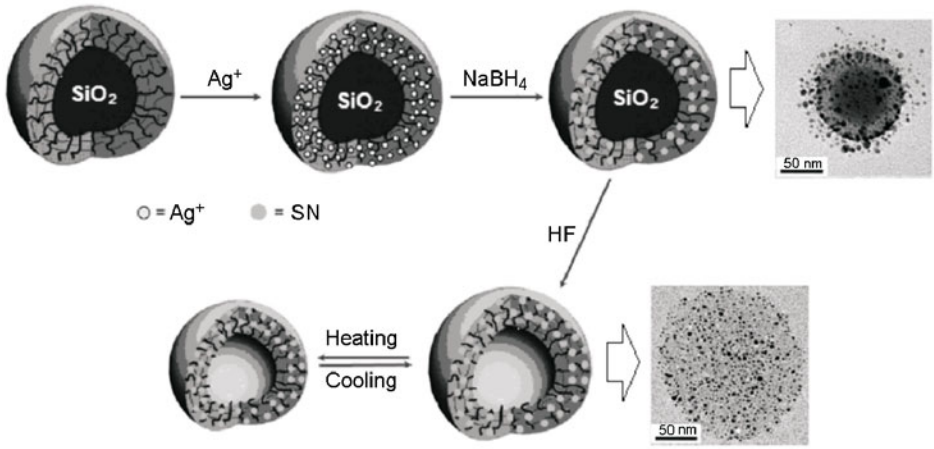

Fig. 3. Scheme for the preparation of thermosensitive hybrid poly(IPAAM)/SN nanocapsules. Reprinted with permission of Wu et al. [55]. Copyright © 2010, American Chemical Society.

Photocatalytically-active hybrid systems are formed by grafting graphene with immobilized SN onto a copolymer of styrene (St) and glycidyl methacrylate [44]. The use of carbon microspheres instead of the copolymer has also been proposed [45]. The use of an epoxide binder for the graphene/silver nanofiber composite filler provides for the formation of electroconducting hybrid systems with a low SN percolation threshold (~10 mass %) [46]. The covalent reaction between the functional groups on the graphene surface and the epoxide groups of the matrix leads to enhanced thermal and chemical stability as well as increased mechanical strength of the nanocomposites. Furthermore, the hybrid nanocomposites derived from silver nanofibers and graphene possess high stability [47], optical transparency (81.5% at 550 nm), and low specific resistance (R = 32.5 Ω·cm) close to R of electroconducting glasses derived from solid In_2O_3-SnO_2 solutions [48]. Polymerization of dopamine on the sensor electrode obtained by the immobilization of SN on a vitreous carbon surface modified with hemoglobin gave nanocomposites with high sensor activity relative to H_2O_2, whose sensitivity may reach $3 \cdot 10^7$ mol [49].

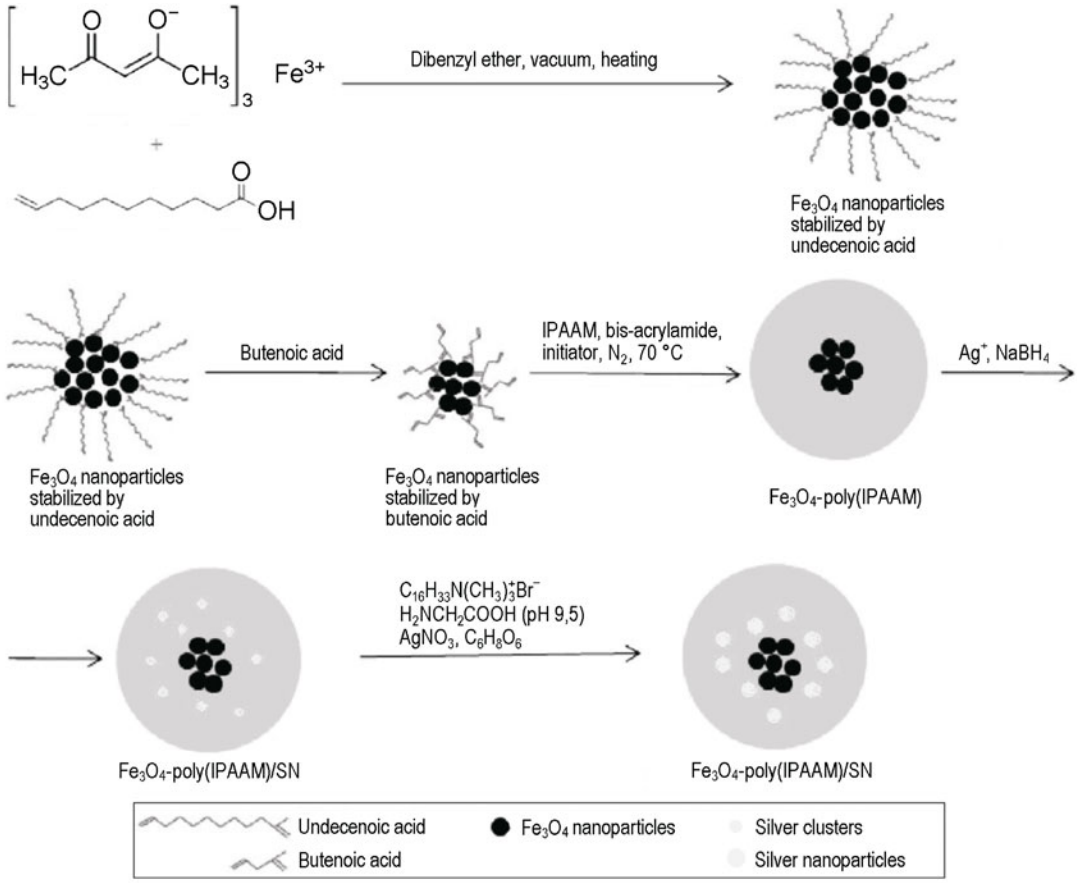

Fig. 4. Scheme for the preparation of hybrid systems derived from Ag and magnetite (Fe_3O_4) nanoparticles immobilized in poly(IPAAM) matrix. Reprinted with permission of Contreras-Cáceres et al. [60]. Copyright © 2011, American Chemical Society.

Polymerization of 4-vinylpyridine (4VP) through the RAFT mechanism [50, 51] on the surface of SiO_2 particles gives hybrid core–shell nanosystems (Fig. 2) [52]. The high affinity of the nitrogen heterocycles in poly(4VP) [52] and the amide groups in polyacrylamide (poly(AAm)) [53] toward silver provides for efficient immobilization of the SN, formed upon the reduction of the Ag^+ ions in the polymer layer, on the surface of highly-dispersed SiO_2. Hybrid composites with bactericidal properties may also be obtained upon the hybridization of SN stabilized by polystyrenesulfonic acid with $CaCO_3$ microparticles [54].

Among synthetic polymers, the products of the polymerization of vinyl (including acrylate) monomers are commonly used. The combination of promising approaches for controlled polymerization and click chemistry gave nanocomposites derived from SiO_2 and N-isopropylacrylamide (IPAAM) or 3-azidopropylacrylamide [55]. Removal of the SiO_2 cores of the hybrid particles gives polymer capsules, in which SN are formed by an *in situ* method (Fig. 3). The SN concentration gradient in the thermosensitive polymer shell of the nanocapsules is a consequence of different density of cross-linking of the macrochains near the inner and outer surfaces of the polymer structures, while the stability of the nanoparticles is attributed to their reaction with the amide groups of the polymer component.

The unique combination of magnetic, chemical, fluorescence, bactericidal properties, and biocompatibility indicates promise for hybrid materials derived from Fe_3O_4 and SN [56-58]. The reduction of Ag^+ ions on the surface of Fe_3O_4 nanoparticles modified with PEG leads to the formation of highly-dispersed hybrid particles for use as a bactericidal filler and biomarkers in magnetic resonance studies [56]. Additional immobilization of lipase enzyme imparts catalytic activity to these nanosystems in the hydrolysis of lipids over a broad temperature and pH range [9, 58]. Polymerization of IPAAM in the

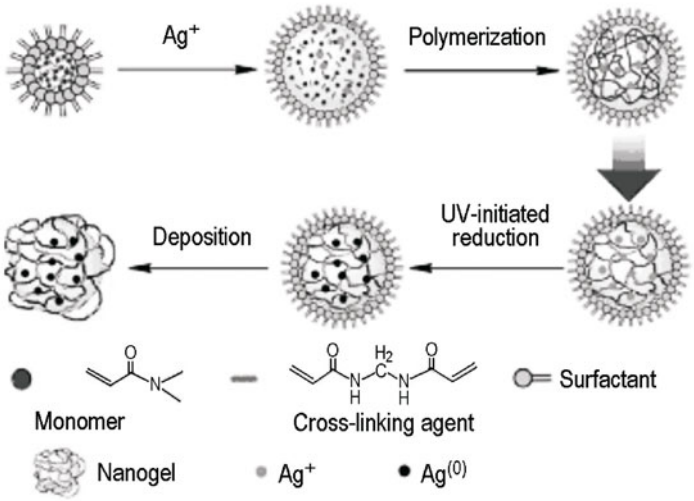

Fig. 5. Preparation of silver-containing hybrid composites derived from N,N-dimethylacrylamide by the inverse microemulsion polymerization method. Reprinted with the permission of Chen et al. [63]. Copyright © 2013, American Chemical Society.

presence of Fe_3O_4 and SN (Fig. 4) gave hybrid sensors for pentachlorophenol and 1-thionaphthalene, whose sensitivity may be varied by changing the temperature of the medium [59, 60].

HYBRID SYSTEMS WITH AN ORGANIC POLYMER MATRIX

Hybrid polymer composites, in which SN are used as the inorganic component, are a very common type of hybrid materials [61-63]. Natural and synthetic polymers of various structure are used for the preparation of these composites and also, when necessary, to impart specific properties of Ag, Au, Pt, or Pd nanoparticles [64-81].

The preparation of SN in a microgel of poly(IPAAM)/carboxymethylchitosan (CMC) modified by maleic acid yields hybrid catalysts for the reduction of 4NT [82]. An analogous method gave composites derived from unsubstituted (AAM) (Fig. 5) [83] and disubstituted acrylamide [63], while the additional introduction of ion-exchange components into the matrix permits efficient controlled variation of the content of stabilized SN [83].

The morphology and catalytic activity of poly(IPAAM)/SN composites may be controlled by altering the extent of cross-linking of the matrix [82, 84]. The rate of reduction of 4NT, which varied in the range 0.124-0.196 $L/m^2 \cdot s$, depends both on the reaction temperature (the lowest reaction rate was noted upon reaching the lowest critical mixing temperature of poly(IPAAM) (34 °C), at which dehydration of the macrochains of the polymer hydrogel occurs) and the size of the SN [82]. High thermal sensitivity is also found for the catalytically-active hybrid microgel obtained by the reduction of Ag^+ ions in the surface layer of the particles of the copolymer of N-vinylcaprolactam and acetylacetoxyethyl methacrylate (Fig. 6) [85]. The temperature dependence of the plasmon properties of these systems indicates a change in the nature of the interaction of the SN with the polymer macrochains. When using the copolymer of IPAAM, acrylic acid (AA), and 2-hydroxyethyl acrylate (HEA), this effect is not observed due to the presence of CO_2H functional groups with high affinity toward silver and lower sensitivity of the polymer matrix to change in temperature [86]. In addition to amide and carboxyl functional groups [82, 86], the terminal dithioester groups of the acrylate matrix, whose presence is related to specific features of its preparation, may participate in formation of the hybrid structure [87].

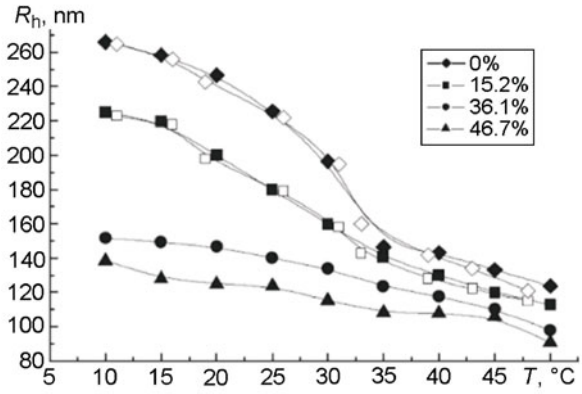

Fig. 6. Temperature dependence of the hydrodynamic radius of the hybrid microgel particles derived from the temperature-sensitive copolymer of vinylcaprolactam and acetoacetoxyethyl methacrylate with SN. Reprinted with the permission of Pich et al. [85]. Copyright © 2006, Wiley-VCH Verlag GmbH & Co., KGaA, Weinheim.

The plasmon resonance (PR) band is shifted toward longer wavelengths upon formation of the hybrid structure of composites derived from a cross-linked polymer of IPAAM and AA with SN [88]. The swelling of the composites in water and an increase in the pH of the medium shift the maximum of the PR band toward shorter wavelengths, indicating partial destruction of their hybrid structure. UV, visible, and Raman spectroscopy indicates pH sensitivity for composites with a matrix possessing semi-interpenetrating polymer networks (semi-IPN) derived from cross-linked poly(IPAAM) and linear poly(AA) [89]. Systems with hydrophilicity, UV adsorption, and catalytic properties dependent on temperature and pH of the medium were obtained *in situ* upon the reduction of Ag^+ ions in the matrix of the copolymer of IPAAM, methacrylic acid (MAA), and AAM [90]. The properties of such hybrid materials permit their use in the preparation of sensors with various sensitivity mechanisms [89, 90].

The use of the poly(AA)/polyethylenimine (PEI) interpolymer complex as the matrix in the radiation chemical preparation of SN showed that the reaction of the CO_2^- groups of the polymer with SN surface leads to the formation of hybrid nanocomposites [81]. Theoretical calculations indicate that the photoactivity of the complexes formed upon the reaction of the polymer CO_2^- groups and silver clusters depends on the electronic structure of the silver atoms [91].

Hybrid composites derived from copolymers of St and its derivatives are also commonly used [34, 83, 84, 92-95]. The deposition of SN on the surface of poly(St) microspheres modified with $ClSO_3H$ gave nanocomposites, in which the SN are stabilized due to their reaction with the SO_3H groups of the polymer matrix [92]. The photochemical reduction of Ag^+ (or Pd^{2+}) ions in the presence of particles of poly(St) or the copolymer of St and IPAAM, containing poly(methylphenylsilane), leads to the deposition of SN on the polymer surface and formation of hybrid catalysts for the reduction of 4NT, whose activity decreases with increasing size of the metal particles [93, 94]. Similar materials may also be obtained by grafting of the polymer onto the SN surface [95, 96]. However, the stability of these materials is diminished even at low SN concentrations (>1 mass %) [95].

The method of preparation of the SN has a marked effect on the structure of the hybrid systems. The introduction of previously prepared SN into a dispersion of particles of the copolymer of St and PEG methacrylate (*ex situ* method) does not lead to the formation of hybrid structure, while the SN are localized in the space between the polymer particles. On the other hand, in the case of *in situ* preparation, a layer of SN is deposited onto the surface of the polymer particles and hybrid structure is formed for the composites [97].

The self-assembly of micelles of block copolymers of poly(isoprene)-poly(AA), poly(St)-poly(4VP) as well as the copolymer of St and 4VP in the formation of hybrid systems was studied by Meristoudi et al. [98]. In media with low polarity,

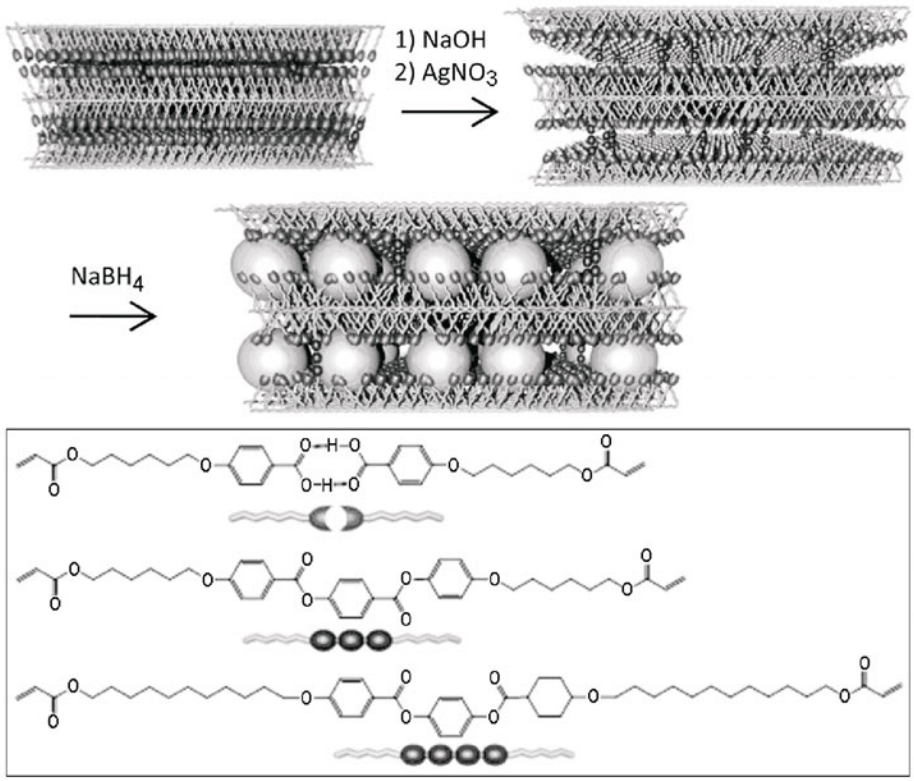

Fig. 7. Formation of SN in the interlay space of a nanoporous matrix of a smectic liquid-crystalline polymer [106]. Copyright © 2013, American Chemical Society.

the formation of SN leads to disappearance of the monomolecular micelles with diameter ~34 nm and to appearance of polymolecular micelles with diameter ~120 nm, which indicates participation of the SN in intermolecular cross-linking during preparation of the nanohybrid systems. The polymer micelles also act as nanoreactors and, by changing their dimensions, we may control the morphology of the SN formed [99]. The deposition of a dispersion of hybrid block copolymer/SN particles onto the surface of a substrate leads to their self-assembly to give cellular coatings, whose properties depend on the polymer concentration, composition of the medium, and nature of the substrate. The use of copolymers with different structures and functionality permits controlled variation of the morphology of the SN as well as the structure and properties of the hybrid composites [98-100]. For example, a high content of siloxane fragments in the structure of the poly(methyl methacrylate)-PDMS block copolymer (poly(methyl methacrylate) = poly(MMA)) imparts enhanced hydrophobicity and thermal stability to its derived nanocomposites but a high concentration (>7 mass %) of SN is required to impart bactericidal activity to these materials [101].

A new method for the controlled variation of the morphology of hybrid systems obtained by deposition of SN onto the surface of a poly(St)-poly(MMA) block copolymer was proposed by Willner et al. [79]. UV irradiation of the poly(St)-poly(MMA)/SN nanocomposite, whose matrix microphase structure consists of cylindrical domains of poly(MMA) with 20 nm diameter, distributed in a continuous poly(St) phase, leads to photodecomposition of poly(MMA) and the partial removal of the attached SN aggregates. In this case, the ester groups of the MMA fragments were found to participate in the reaction with the SN, even though the energy of the Ag···RO_2C bond is rather low [79, 101]. Depending on the chemical structure of poly(MMA) and the method of its preparation, other functional groups may participate in formation of the hybrid structure. In particular, the formation of the Ag—S bond with strength >200 kJ/mol [102] was noted in the formation of composites derived from SN and a poly(St)-poly(MMA) block copolymer obtained by RAFT polymerization [70]. In the latter case, the terminal dithiobenzoate groups of poly(MMA) (these groups are present due to use of dithioesters as the chain transfer agents) [70, 104] undergo a polymer-like transformation through reaction with *n*-butylamine to give a polymer with terminal

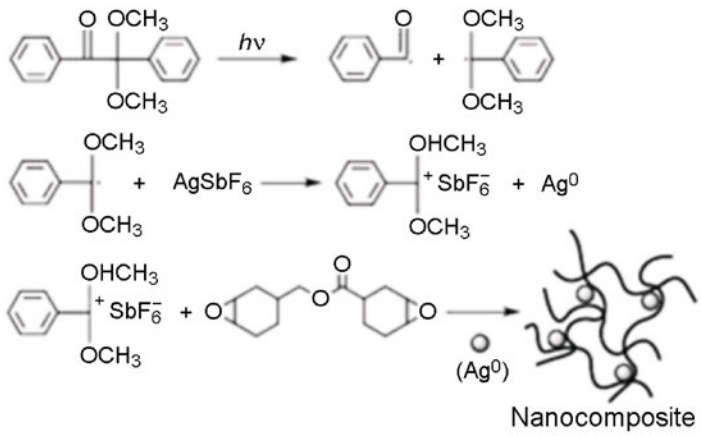

Fig. 8. Photoinitiated *in situ* preparation of hybrid nanocomposites in the case of epoxide polymer/SN systems. Reprinted with the permission of Yagci et al. [115]. Copyright © 2009, FSCT and OCCA.

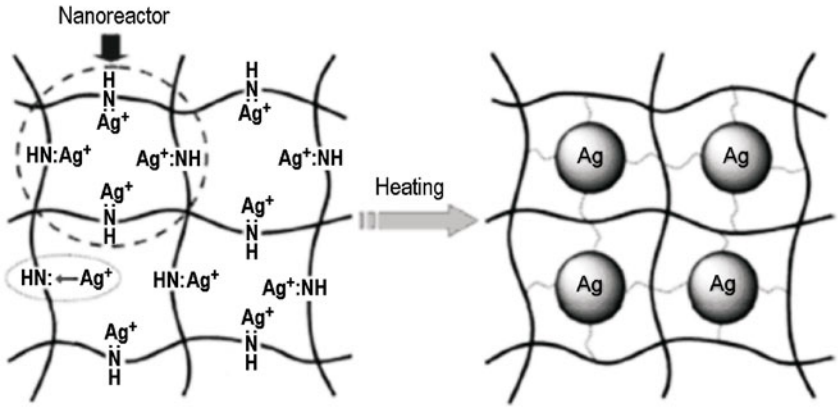

Fig. 9. Scheme for formation of SN in nanodimensional cavities of a reactive polymer matrix. Reprinted with the permission of Zhang et al. [121]. Copyright © 2013, American Chemical Society.

SH groups having high affinity for silver. Such hybrid systems have good electrical conductance [79], optical properties [103], and bactericidal activity [70, 103], while the introduction of $NaYF_4$ particles doped with Yb^{3+} and Er^{3+} ions and their reaction with the SN impart luminescent properties to these materials [105].

Nanoporous systems, whose organic phase is a smectic liquid-crystalline polymer network formed upon the copolymerization of 4-(6-methacryloylhexamethylidene)benzoic acid and various diacrylates, were studied by Dasgupta et al. [106]. The preparation of these nanocomposites was carried out by destruction of the interlayer hydrogen bonds of the copolymer matrix due to swelling in buffer solution with subsequent introduction of Ag^+ ions into the hydrogel and reduction of these ions (Fig. 7). The formation of a hybrid structure in these systems occurs due to reaction between the SN and deprotonated CO_2H groups of the copolymer (the mechanism of the reaction of the surface layer of silver atoms with low-molecular-weight organic compounds (aliphatic and aromatic acids) [107-109] as well as polymers containing CO_2H groups [110] has been studied in detail by Kilin et al. [109]; the energy of this interaction may reach 58 kJ/mol [109]). The interlayer space of the polymer matrix controlled by the structure of the acrylic monomers used provides relative elasticity for these materials and acts as a nanoreactor for the formation of SN.

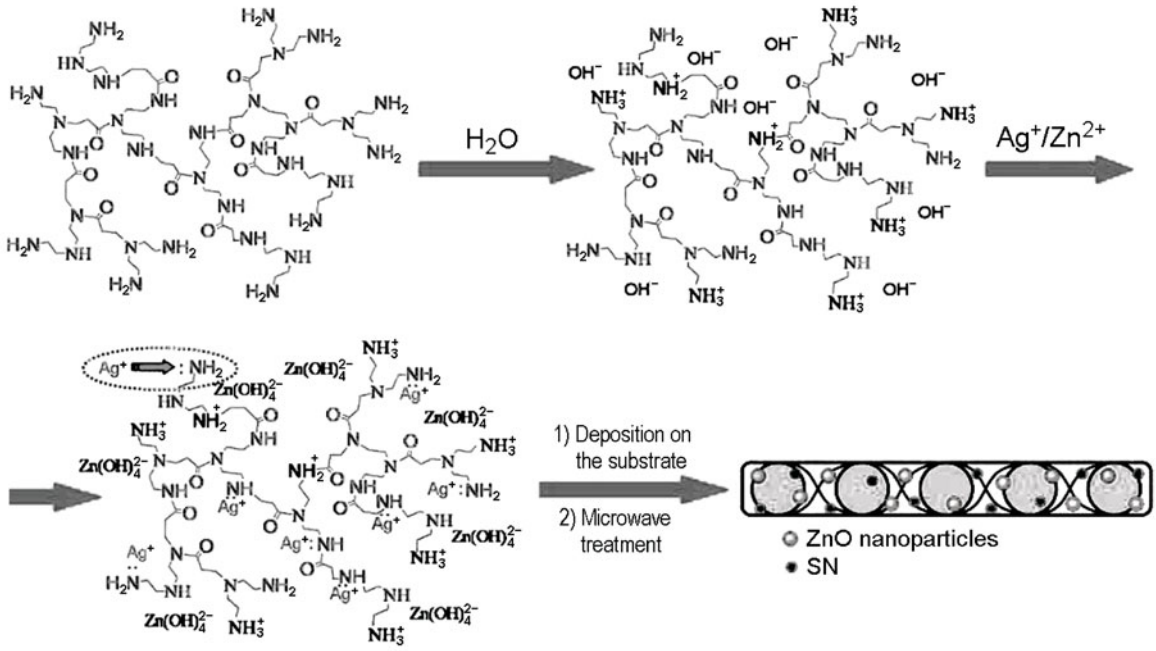

Fig. 10. Preparation of hybrid composites containing silver and zinc oxide nanoparticles and derived coatings. Reprinted with the permission of Zhang et al. [125]. Copyright © 2013, Wiley Periodicals, Inc.

Hybrid nanosystems derived from PVA or polyvinyl acetate and SN obtained *in situ* have bactericidal and sensor activity [111-114]. The template synthesis of analogous composites based on the self-assembly of PVA macromolecules with grafted *o*-dihydroxybenzene fragments to give a three-dimensional, highly-porous structure and participation of the phenol groups of the matrix in the reduction of Ag^+ ions yields sensor and catalytically-active materials [113].

The use of a complex initiator, namely, 2,2-dimethoxy-2-phenylacetophenone/$AgSbF_6$, whose photolysis gives SN, free radicals, and cations (Fig. 8) permits the initiation of the polymerization of unsaturated monomers and epoxide compounds as well as formation of hybrid systems with various properties [115]. Silver particles or nanoparticles after modification of their surface with $H_2N(CH_2)_3Si(C_2H_5)_3$, can also be used for the curing of epoxides [116]. The bifunctionality of the $AgNO_3$/ethylene glycol oxidation–reduction system, which acts both as an initiator in the polymerization of N-vinylpyrrolidone (VP) and as a precursor of SN, permits optimization of the method of preparation of hybrid nanocomposites [117]. The polymerization of vinyl cinnamate in the gas phase and the reduction of Ag^+ ions yield hybrid poly(vinyl cinnamate)/SN composites [118].

The formation of composites derived from SN and π-conjugated poly(*p*-phenylenethynylene) (PPE) is accompanied by a shift of the maximum of the fluorescence band of PPE toward lower λ and band narrowing. This behavior is related to conformational transformation of the PPE macrochains and the contribution of the PR of the nanoparticles to the energy characteristics of the matrix fluorescence [119].

Heterochain nitrogen-containing polymers such as polyurethane (PU), polyamides, polyamidoamines (PAdAm), and polyimides (PI) are commonly used in the preparation of silver-containing hybrid nanosystems. Due to reaction of Ag^+/SN with nitrogen- and oxygen-containing functional groups of the polymer, these composites show a homogeneous distribution of the dispersed phase in the polymer matrix, improved mechanical properties, and thermal stability [120].

The reduction of Ag^+ ions within the polymer complex with amphiphilic PAdAm obtained by the amidation of PEI using palmitic acid gives composites, which display bactericidal properties when the specific concentration of SN is ~10^{-6} g/cm^2 [62]. The small diameter of the SN (≤3 nm) formed in the PAdAm globules is attributed to efficient reaction of the silver ions (and/or clusters) with the functional groups of the matrix (Fig. 9) in a broad concentration range (the Ag^+/N ratio

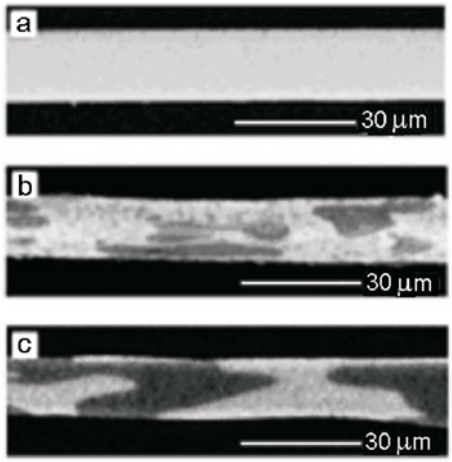

Fig. 11. Microphotographs of a cross-section of electroactive hybrid systems derived from various PI and SN (the superscript indicates the mole ratio of the structural fragments of the composites): a) $(DBTA/TDA)^{100}/SN^{40}$, b) $(DBTA/TDA)^{70}/(DBTA/TPDB)^{30}/SN^{40}$, c) $(DBTA/TDA)^{50}/(DBTA/TPDB)^{50}/SN^{40}$. Reprinted with the permission of Yorifugi et al. [128]. Copyright © 2010,Wiley-VCH Verlag GmbH & Co., KGaA, Weinheim.

ranged from 1/64 to 1/2) [121, 122]. In the case of a large excess of Ag^+ ions or the use of PAdAm, the structure of which is conducive to localization of the nitrogen-containing groups on the outer surface of the globules, the kinetic control of SN diminishes, leading to the formation of nanohybrids with polydispersed SN with diameter 30-200 nm [121]. The protonation of the NH_2 groups dependent on the pH of the medium and reactive additives to such systems are capable of altering the morphology of the nanodispersed metallic phase [123].

The reduction of Ag^+ ions in the presence of PAdAm, amidated thioglycolic and perfluorocarboxylic acids permits the preparation of hybrid fillers for imparting bactericidal properties to PU composites [124]. The presence of perfluoroalkyl and thiol-containing substituents in the structure of PAdAm provides for a gradient of the SN concentration in PU composites (the SN concentration on the PU surface may be 5-7 times greater than the SN concentration in the bulk). The reaction of Ag^+ and Zn^{2+} ions, and PAdAm in solution leads to a precursor, containing both the $[Zn(OH)_4]^{2-}$ hydroxo complex and $(Ag^+)_n$PAdAm polymer complex (Fig. 10). Heat treatment of this precursor gives a nanostructurized PAdAm/SN/ZnO coating with bactericidal and UV-absorbing properties [125]. Modification of PEI by ferrocene (FC) also facilitates the formation of hybrid nanosystems [126]. FC, which possesses high chemical stability and electron donor properties, provides for a low rate of reduction of Ag^+ ions, while an amino-containing matrix facilitates formation of SN with low polydispersion. The practical value of such materials is related to the strong tendency of the matrix to form conjugates with various biomacromolecules.

Heat-stable hybrid materials may be obtained using PI as the polymer matrix [127, 128]. The deposition of silver hexafluoroacetylacetonate on a layer of polyamidoacid (PAdA) derived from 2,2-bis(3,4-dicarboxyphenyl)hexafluoropropane dianhydride and 2,2-bis[4-(4-aminophenoxy)phenyl]hexafluoropropane with heat treatment at 300 °C gave composite coatings with high reflectivity [127]. The reaction of SN with the CO_2H groups of PAdA not utilized to form the PI matrix leads to the formation of the hybrid structure of the composites and homogeneous deposition of the nanoparticles on the PI surface. The prior preparation of PI prevents formation of a homogeneous SN layer and hybrid systems due to reduced reactivity of the amide groups and rigid structure of the matrix macrochains. Hybrid systems with good heat conductance are obtained by introducing SN into the PI matrix with alternating segments of 3,3′,4,4′-diphenyltetracarboxylic acid (DBTA)/ 4,4′-thiodianiline (TDA) and DBTA/2,2′-bis(trifluoro)-4,4′-diaminobiphenyl (TFDB) [128]. The strong microphase separation in the composites and the affinity of the DBTA/TDA segments for silver (probably due to the sulfur-containing groups) leads to the predominant distribution of SN in the phase enriched in DBTA/TDA and aggregation of SN in the

continuous phase (Fig. 11). Such composite structure provides for thermoplasticity up to $2.1 \cdot 10^{-7}$ m^2/s as well as enhanced heat stability and elasticity.

The oxidative polymerization of amines in the presence of Ag^+ ions can also lead to multifunctional hybrid systems. The polymerization of aniline (An) in the presence of Ag^+ ions gave poly(An)/SN nanocomposites with electrical conductance subject to controlled variation as well as UV-absorbing and photoluminescent properties [129]. The use of substituted anilines as comonomers improves the heat stability of the nanocomposites but decreases their conductivity [130]. Replacing poly(An) on polypyrrole decreases the stability of nanocomposites, which leads to a high degree of SN aggregation [131, 132]. The enhanced adsorption capacity relative to Ag^+ ions (up to $1.85 \cdot 10^{-2}$ mol/g with adsorption efficiency >99.98%) and reducing activity of the copolymer of An and 5-sulfo-2-anisidine may be used for the preparation of conducting composites and adsorbents for the concentration and separation of silver from waste water [133]. The formation of a layer of SN on the surface of fibers of the interpolymer complex poly(*o*-methoxyaniline)(PoMA)/ribonucleic acid (RNA) imparts semiconductor properties to the composites, which is attributed to features of the charge transfer between the matrix and SN [134]. PoMA in such systems acts as a reducing agent for Ag^+ ions and a stabilizer for SN.

Electroactive hybrid composites may also be obtained by means of the oxidative polymerization of sulfur-containing heterocyclic compounds such as thiophenes. The immobilization of SN in a polythiophene layer on the surface of vitreous carbon may be used to obtain multilayer composites with enhanced conduction [135]. Composites with conductivity reaching 1.25 S/cm due to efficient charge transfer between SN and the matrix were obtained by the polymerization of 3,4-ethylenedioxythiophene in an aqueous solution of $AgNO_3$ acting as a cooxidizing agent [136]. Nanocomposites derived from poly(3-hexylthiophene), [6,6]-phenyl-C_{61}-butyl butyrate, and SN obtained *in situ* have been used for the preparation of electrodes in solar cells with efficiency reaching 4.3% [137].

The dispersion of MCNT-SN composite filler obtained dy immobilization of SN on the surface of MCNT modified with $C_6H_5CH_2SH$ as a biphilic spacer and silver microparticles (SM) in polyvinylidene fluoride (PVDF) leads to the formation of electroconducting hybrid polymer coatings [138]. These materials are efficient deformation sensors since their conductance drops from 5710 to 20 S/cm with deformation from 0% to 140%. Stronger microphase separation and a deterioration of the properties of the hybrid systems is noted from SM concentration above 8.6 mass %. The replacement of SN by poly(An) in the modification of the MCNT surfaces reduces the conductance and sensor activity of the composites [139].

Other properties of composite fillers in hybrid systems may be improved in addition to electrical conductance. The cation-exchange groups of the SiO_2-containing mineral, bentonite, permit the introduction of SN into its structure, while the resultant hybrid filler upon its introduction into polymers such as poly(MMA) due to partial exfoliation imparts strong bactericidal activity [140]. Nanocomposites obtained by the introduction of $BaTiO_3$ with immobilized SN into a matrix of PVDF have dielectric susceptibility ε more than thrice higher than ε of systems derived from the initial $BaTiO_3$ [141], while the deposition of highly dispersed CdSe modified with PEG imparts luminescent properties to composites [142].

The use of polyethers in the preparation of hybrid systems is attributed to weak reducing properties of the oxyalkylene fragments and strong stabilizing activity relative to SN [143]. Nanocomposite catalysts were obtained *in situ* by the preparation of SN in the matrix of the triblock PEG-polypropylene glycol-PEG copolymer with subsequent introduction of α-cyclodextrin (α-CD) into the reaction system [144]. As an efficient reducing agent of Ag^+ ions, the block copolymer forms guest–host supramolecular aggregates with α-CD. However, in the presence of SN, this interaction is much weaker due to interaction of the PEG macrochains with the nanoparticle surface. Nanohybrids with magnetic and fluorescent properties are formed upon the introduction of SN into the polyisoprene-PEG block copolymer acylated with α-lipoic acid, whose —S—S— terminal groups provide for a covalent bond between the matrix and the SN [145].

Among the natural polymers, polysaccharides are commonly used for the preparation of hybrid composites. The OH and CO_2H groups of polysaccharides may participate both in the reduction of Ag^+ ions and stabilization of SN. Upon the deposition of chitosan and SN acting as physical cross-linking sites, whose presence enhances the elasticity and decreases the hydrophilicity of these systems [146], biocompatible multilayer coatings with enhanced mechanical strength and marked bactericidal activity for specific SN concentration $<2 \cdot 10^{-5}$ g/cm^2 are obtained on an inert base [147]. Composites with enhanced mechanical properties and thermal stability may be prepared using a mixed polymer matrix derived from the polysaccharide, pullulan, along with PVA and SN [148]. The resistance of composite chitosan/PEG/SN fibers, whose enhanced bactericidal activity is imparted by chitosan and SN (photoactive TiO_2 may also be introduced into the composite

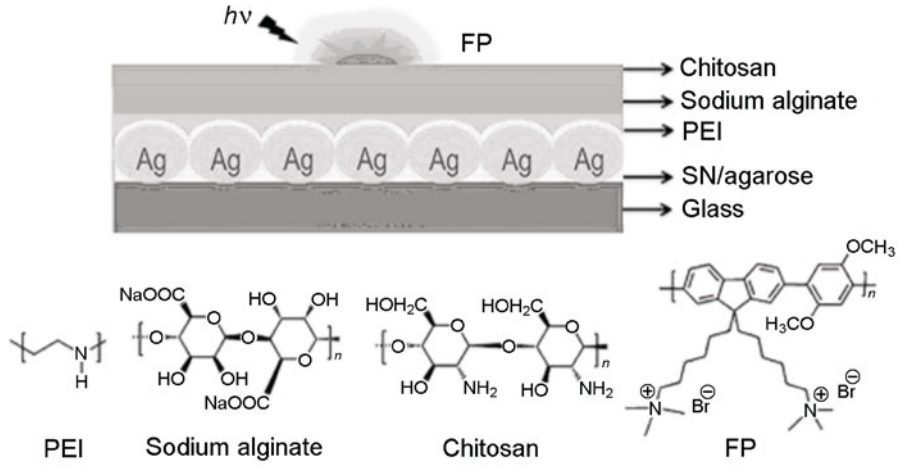

Fig. 12. Structure of multilayer hybrid coatings with enhanced fluorescence characteristics. Reprinted with the permission of Wang et al. [154]. Copyright © 2014. Rights managed by Nature Publishing Group.

[149]), to the action of aqueous media may be considerably enhanced upon cross-linking with glutaraldehyde [150]. Spectral studies of these composites indicated a different type of interaction between the SN and organic components of these systems due to the presence of various functional groups. The presence of SN may alter the phase structure of composites derived from chitosan and gelatin, which is noted in improved mechanical properties and more rapid separation of low-molecular-weight additives (in this case, a drug component, metronidazole) into the external medium [151]. Silver clusters stabilized by the chitosan/poly(AA) polymer matrix impart high sensor sensitivity (down to 10^{-9} mol/L) toward organic disulfides [152]. The chemical mechanism of the sensor activity is related to the formation of Ag—S bonds upon the hemolytic decomposition of the —S—S— bonds in the presence of highly-dispersed silver, while sensors for glucose and its polymers with sensitivity down to $5 \cdot 10^{-5}$ g/L were obtained by the immobilization of β-glucanase enzymes (glucose oxidases) in the chitosan/galactomannan/SN hybrid system [153]. Multilayer hybrid systems with strong fluorescence are formed in by the deposition of layers of SN/agarose, PEI, sodium alginate, chitosan, and poly[9,9′-bis(6"-(N,N,N-trimethylammonium bromide)hexylfluorene-2,5-dimethoxy-1,4-phenylene)] (FP) on a glass plate (Fig. 12) [154]. Varying the SN concentration in the composite structure may improve the fluorescent properties, while additional immobilization of the tyrosinase enzyme in the surface layer imparts sensor activity toward phenols (the sensitivity toward bisphenol A reaches 10^{-8} mol/L).

The reducing properties of the matrix are used in the preparation of SN/starch hybrid capsules by inverse emulsion [155]. The partial oxidation of the surface of the capsules improves their adhesive properties. Agarose also possesses reducing activity, while the efficiency of the stabilization of SN in the agarose/SN system is related to the presence of OH and CO_2H groups in the polymer [156]. The invariance of the UV and visible absorption spectra of these composites despite varying their composition indicates efficient SN stabilization through an analogous mechanism [157].

The structure of the nucleic acids (RNA and deoxyribonucleic acid (DNA)) and the presence of fragments of heterocyclic compounds (nitrogen bases) in these acids, whose nitrogen atoms have high affinity for silver, permits their use in the preparation of hybrid nanocomposites with valuable properties [64, 78, 134]. Computer modeling has shown the possibility of obtaining luminescent nanomaterials from DNA and silver clusters, whose properties depend on the structure and composition of the composites [158]. Special importance is found for the energy of the interaction of the structural fragments of the DNA macromolecules and silver atoms. In particular, the energy of the interaction of silver with C=O groups of the nitrogen bases does not exceed 95 kJ/mol, while this parameter in the formation of chelate structures may reach 413 kJ/mol. The theoretical modeling results were experimentally supported in a study of hybrid nanoparticles prepared from silver clusters with a shell consisting of DNA macromolecules compacted by polyallylamine [159]. The polymer shell protects the silver clusters from solvation and oxidation and also provides stability for the structure and luminescent properties of the composites

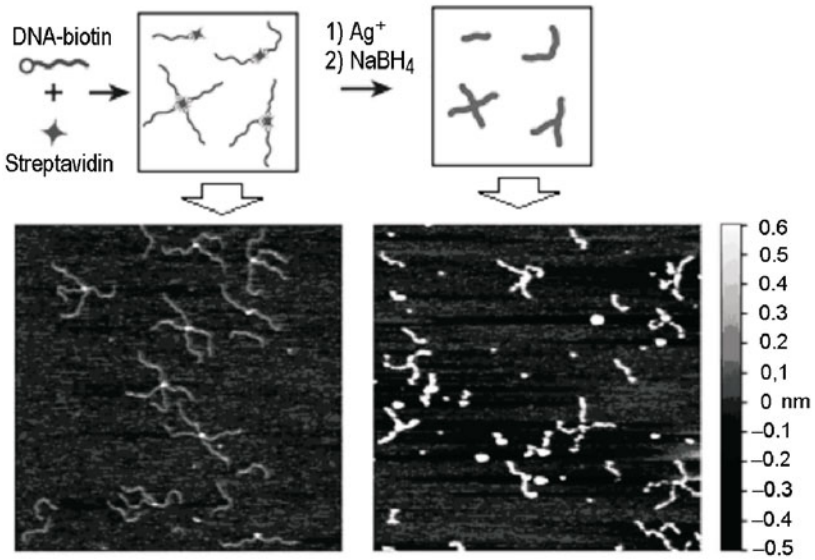

Fig. 13. Star-shaped hybrid nanostructures obtained by the deposition of SN onto DNA-streptavidin interpolymer biocomplexes. Reprinted with the permission of Rudiuk et al. [161]. Copyright © 2013, Royal Society of Chemistry.

(emission bands with maxima ~590 and ~680 nm at λ_{exc} = 280 nm). The similar hydrodynamic radius of the compacted DNA globules and their derived nanocomposites (150 ± 50 nm) indicates efficient packing of the hybrid structures as the result of interactions of the silver clusters with functional groups of the nitrogen bases of the DNA macrochains. Modification of DNA molecules with biotin imparts high affinity for the protein, streptavidin, while the deposition of SN on streptavidin-DNA self-aggregates (streptavidin may bind up to four DNA macromolecules) permits the preparation of hybrid polymer nanosystems (Fig. 13) [160, 161]. The mean length of the DNA branches upon the deposition of SN on them is reduced from 174-181 to 60-68 nm due to conformational transformations of the DNA macrochains upon their interaction with SN [161].

According to Dawn and Nandi [162], the formation of SN during the preparation of bionanocomposites derived from DNA, PoMA, and $AgNO_3$ with broad-band semiconductor properties should be attributed to localization of electron density on Ag^+ ions upon the interaction of these bionanocomposites with PoMA [162]. A study of the electrical conductance of the hybrid systems showed high energy for the bond between SN and PoMA, while the interaction between DNA and the PoMA/SN system is electrostatic in nature.

Intensive work is now underway in an attempt to obtain bionanocomposites derived from proteins or their low-molecular-weight analogs (peptides) and SN [163, 164]. The interaction of the amino-containing structural units in the protein, bacteriorhodopsin (bR), namely, cysteine, arginine, lysine (polylysine) with SN [165, 166] leads to a shift of the PR band toward longer wavelengths ($\Delta\lambda$ depends on the structure of the amino-containing spacer) along with an increase in the intensity of this band by 4%-26%, which permits us to use these composites as sensitizers for photochemical reactions [167]. Detailed studies of such systems have shown that the presence of NH_2 [61, 168] or CO_2H groups [169] in protein macromolecules is conducive for the formation of hybrid structure without the introduction of additional reactive compatibilizers. The combined presence of NH_2 and CO_2H groups in proteins provides for stability of the SN in the hybrid systems when their concentration is >6 mass % [170]. Aggregates with hybrid structure and molecular mass (MM) ~$2.5 \cdot 10^5$ are formed upon the interaction of SN and oligopeptides with N- and O-containing functional groups (MM ≈ $6.5 \cdot 10^3$) obtained by hydrolysis of keratin [164].

Sulfur-containing thiol and disulfide groups and heterocyclic fragments of protein molecules containing electron-donor atoms may also interact with SN. Raman spectroscopy indicates that the interaction between peptide molecules and SN in L-lysine–L-lysine–L-cysteine/SN nanosystems is due to the formation of Ag—S bonds. The aminoalkyl groups

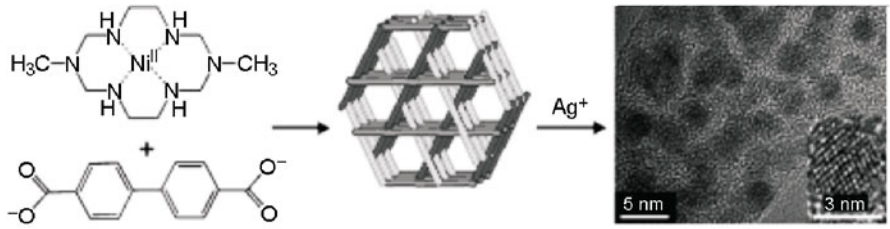

Fig. 14. Scheme for preparation of monodisperse SN (diameter ~3 nm) in the matrix of CP with zeolite-like porous structure. Reprinted with the permission of Moon et al. [188]. Copyright © 2005, Wiley-VCH Verlag GmbH & Co., KGaA, Weinheim.

form an outer shell of hybrid particles, which is sensitive to the acidity of the medium [171]. At pH ≈ 2.3, such systems form stable dispersions with particle diameter 23 ± 13 nm, while up to 10 particles aggregate in the structure with increasing pH with diameter 875 ± 108 nm. Modification of oligoglycine with 1,10-phenanthroline stabilizes SN and facilitates the formation of sensor- and catalytically-active hybrid systems, while the presence of substituents in the structure of the heterocyclic modifier suppresses the capacity of oligoglycine to form hybrid composites [172]. The interaction of chromophore groups of amino acid fragments of peptides in silver clusters, which affects the optical properties of the hybrid systems [173], has found practical use in the preparation of hybrid biomarkers for the visualization of histidine-containing proteins in biochemical research [174]. Protein macromolecules containing tyrosine (2-amino-3-(4-hydroxyphenyl)propionic acid) fragments may reduce Ag^+ ions due to the phenolic OH groups according to the following scheme:

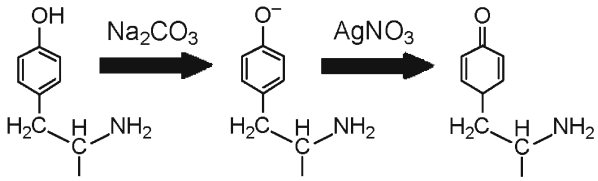

and affect the kinetics of SN growth, which permits the formation of nanostructures of given shape and size [176].

Attention is now turning toward hybrid systems derived from SN and biomacromolecules capable of self-assembly to give nanotubes [176, 177], virus-like particles [178], and viruses [179]. Filling the cavities of nanotubes formed upon the self-assembly of peptide molecules possessing specific structure with silver permits us to obtain composites with unique electrical conductance and electromagnetic properties [176, 177]. Similar systems were obtained upon the deposition of metal nanoparticles on the surface of viruses [180]. Hybrid composites obtained upon the deposition of SN onto the surface of tobacco mosaic virus has higher electrical conductance than for single-walled carbon nanotubes [181]. Further detailed analysis of the interaction of associates of protein macromolecules and SN will lead to understanding of the electrochemical processes in such systems with the aim of improving their electrical properties.

SILVER-CONTAINING COORDINATION POLYMERS

There has been considerable recent interest in the synthesis and study of silver-containing hybrid systems, which are coordination polymers (CP) featuring bonds between the silver atoms (d^{10}–d^{10} interaction) such that di-, tri-, tetra-, and octameric metal clusters as well as polymer chains $(Ag)_n$ are formed [182-185].

Hybrid systems derived from organometallic compounds with polymer structure containing clusters or SN have been obtained by various workers [186-188]. The highly-porous CP obtained using the hexaazamacrocyclic complex of Ni^{2+} ions and sodium 4,4′-biphenyldicarboxylate play a structurizing role in the synthesis of SN (Fig.14) [188]. Hybrids derived from the

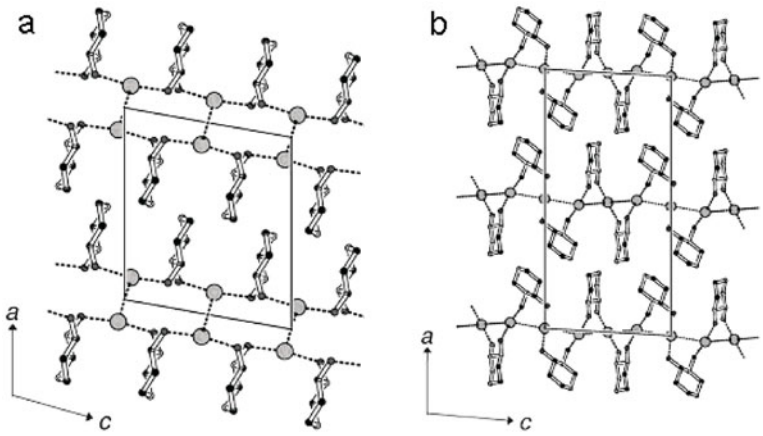

Fig. 15. Fragments of CP macrochains with dimeric (a) and polymeric silver clusters (b). Reprinted with the permission of Kalf et al. [196]. Copyright © 2006, Royal Society of Chemistry.

complex [Ni(1,4,8,11-tetraazacyclotetradecane)$_2$(1,1′-biphenyl-2,2′,6,6′-tetracarboxylic acid)]$_n$ and SN were prepared analogously [187]. In both cases, Ni^{2+} ions act as the reducing agents.

The polymer complex $[Ag_2L(CF_3CO_2)_2]_n$ (where L = 2-(2′-pyridyl)quinoxaline) with linear structure was obtained by Bi et al. [189]. The length of the Ag—Ag bond ($l_{Ag\text{-}Ag}$) in the Ag_2 clusters is 3.06 Å. This value is less than the sum of the van der Waals radius of silver atoms (the maximum distance, at which electrostatic interaction is possible, is 3.44 Å [190, 191]), but exceeds $l_{Ag\text{-}Ag}$ in the metal (2.88 Å) [192]. Two- (2D) or three-dimensional (3D) supramolecular structures are formed in the complex of 1,2-bis(3′-pyridyl)ethyne and Ag^+ ions; $l_{Ag\text{-}Ag}$ between the macrochains of the CP is 3.30 Å, which indicates a weak interaction between the metal atoms due to coordination of the electron-donor groups of the ligand [193]. However, even the weaker interaction between silver atoms ($l_{Ag\text{-}Ag}$ > 3.44 Å) in the Ag^+-bipyridyl complex permits formation of supramolecular 3D structures [194].

Hybrid systems derived from the Ag_2CA complex (where CA is cyanuric acid) are hydrogen-bonded alternating layers of silver atoms. This structure accounts for unique anisotropic electrical conductance (the conductance parallel and perpendicular to the silver layer differs by a factor of 250) to the CP along with dielectric properties (the dielectric constant ε of the CP at 27 °C is $2.2 \cdot 10^4$, which is comparable to ε for $BaTiO_3$ ($1.2 \cdot 10^4$)) [195].

An interesting structure was noted for CP obtained from 1,2-diaminocyclohexane and $AgBF_4$ or $AgNO_3$ [196]. Depending on the reaction conditions during the preparation of these polymer complexes, we may obtain either dimeric Ag_2 ($l_{Ag\text{-}Ag}$ = 3.11 Å) or polymeric $(Ag)_n$ clusters with different $l_{Ag\text{-}Ag}$ between adjacent metal atoms (3.12 and 3.27 Å) (Fig. 15). The formation of $(Ag)_n$ is also characteristic for the supramolecular 3D structure of the polymer complex $[(N(C_2H_5)_4)_3(Ag_6I_9)]_n$ [197].

Formation of 3D structures in CP from derivatives of imidazole and Ag^+ ions also occurs due to a weak interaction between the Ag atoms ($l_{Ag\text{-}Ag}$ = 3.12-3.27 Å) and hydrogen bonding between the heterocycles [198]. The bulky substituents in the ligand may destroy Ag—Ag bonds. Analogous CP are formed upon the interaction of silver salts and substituted pyrazoles: $l_{Ag\text{-}Ag}$ in this case between adjacent silver atoms in the macrochains (3.37-3.40 Å) is greater than $l_{Ag\text{-}Ag}$ between metal atoms in adjacent macrochains (3.25-3.27 Å) [199]. Composites obtained upon the introduction of CP into a polyethylene matrix have strong luminescence with λ_{max} = 520 nm due to Ag→ligand and intracluster Ag→Ag charge transition (*d–s/d–p* transition) as well as strong bactericidal activity [200]. CP with ladder or spiral structure are formed upon self-assembly of complexes of carboxyl-containing pyrazoles [201], while the metal atoms are associated in linear Ag_4 subunits, in which $l_{Ag\text{-}Ag}$ does not exceed 3.23 Å [202].

Unique properties are found for CP obtained from Ag_2O and 4-fluorobenzoic acid (FBA), 1,1-cyclopentanedicarboxylic acid (CDA), or iminodiacetic acid (IDA) [203]. An X-ray crystallographic study showed that the $(Ag\text{-}FBA)_n$ and $(Ag_2IDA)_n$ CP consist of Ag_2 clusters with $l_{Ag\text{-}Ag}$ = 2.85 and 2.93Å, respectively. Ag_4 clusters are characteristic for the structure of $(Ag_2CDA)_n$ with $l_{Ag\text{-}Ag}$ = 2.79-2.99 Å. The Ag—Ag bond (2.79 Å) is the strongest bond between silver atoms among reported silver compounds, including the metal. These complexes have extremely high cytotoxicity for all types of living cells.

The self-assembly of complexes formed in the reaction of $AgNO_3$ and pyridine derivatives may occur to give hybrid CP both by means of Ag—Ag bonds [204] and due to hydrogen bonding between the ligands and the NO_3^- counter-ions in the silver salts [205]. The supramolecular structure of the CP significantly affects the nature of the thermal decomposition of these species. Stabilization of the silver clusters in the matrices of various CP may be achieved by means of nitrogen- [206, 207] and silver-containing ligand functional groups [208]. The strength of this interaction and the structural features of the heterocyclic ligands impart enhanced thermal stability [205, 208] and luminescent properties [200, 208] to these hybrid systems, while the use of thermolabile ligands such as *o*-sulfobenzimide and substituted ethylenediamine reduces the heat resistance of these systems [209].

New CP with 3D structure, whose macrochains consist of alternating structural fragments of two types (type A and type B), are obtained using 1,3,5-benzenetricarboxylic acid (BTA) as the ligand [210]. Fragments A contain Ag_2 clusters with $l_{Ag\text{-}Ag}$ = 2.98 Å stabilized by a system of two bidentate and one monodentate CO_2^- ions (an analogous type of coordination of the Ag_2 subunits is found for the CP derived from $AgNO_3$ and 3-aminobenzoic acid [211]). Fragments B have a more complex structure, in which linear Ag_4 clusters are stabilized by a system of Ag—O and Ag—Ag bonds. An interaction between structural fragments A and B arises by means of an Ag—Ag bond, which results in the formation of $(Ag)_n$ polymer chains. The structure of the hybrid CP provides for electrical conductance upon to $1.06 \cdot 10^{-6}$ S/cm as well as semiconductor and luminescent properties (λ_{max} = 460 nm for λ_{exc} = 360 nm). Ag_3 subunits also impart luminescent properties to CP from the $[Cu(1,3\text{-diaminopropane})_2][Ag_3(CN)_5]$ complex (λ_{max} = 495 nm for λ_{exc} = 313 nm) [212].

The supramolecular assembly of the complex obtained from $AgNO_3$, Dy_2O_3, and nicotinic acid leads to the formation of hybrid CP with three-dimensional structure and porosity analogous to zeolites, while the Ag_2 clusters and heterometallic nature of this complex imparts luminescent properties to the CP [213].

Multifunctional hybrid systems may be obtained from SN and complexes of other metals, using their reducing [214] and stabilizing properties [214, 215]. Synergism of plasmon [216, 217] and photosensitizing properties [218, 219] is characteristic for composites derived from associates of complex molecules with SN deposited on their surface. The sensitivity of the luminescent properties of the hybrid systems to microamounts of oxygen suggests their use as oxygen sensors [215].

CONCLUSION

Analysis of the literature shows that the use of modern methods of synthesis and modification of low- and high-molecular-weight compounds, broad variation of the chemical structure of natural and synthetic polymers, and the use of their reducing properties and capacity to undergo self-assembly permit us to obtain multifunctional silver-containing polymer composites with hybrid structure.

The chemical and phase structure of the polymer matrix upon the introduction of nanodispersed silver provides for stabilization of metal nanoparticles by formation of covalent and hydrogen bonds or ion–dipole, dipole–dipole physical bonds and for the contribution of the intrinsic properties of the components to the final properties of the composites. By altering the chemical structure of the polymer component, we may enhance its adsorption capacity toward ions and the stabilizing effect relative to silver nanoparticles as well as control the distribution of the nanodispersed filler in the composite matrix.

Organo–inorganic hybrid matrices hold great interest for use in both research and practical applications. These matrices combine the properties of both the organic (mechanical strength, elasticity, lyophilicity and transparency) and inorganic components (hardness, rigidity, thermal stability, thermal conductance, and electrical conductance). Silver nanoparticles impart their specific bactericidal, plasmon, and luminescent characteristics to these composites. The immobilization of metal nanoparticles on the substrate surface provides for stabilization of the nanodispersed component and

improved heat conductance, electrical conductance, and luminescent characteristics of the functional substrate. When using nanodispersed silver as an independent inorganic component of hybrid systems, this metal provides sites for physical cross-linking between the polymer macromolecules also enhances the mechanical properties of the resultant hybrid materials. The abovementioned synergism of the properties of the silver nanoparticles and polymer component has a positive effect on the resultant characteristics of the hybrid systems obtained.

Separate attention should be given to silver complexes, which, depending on the chemical structure of the ligands, form various coordination polymers. Silver atoms structurized in clusters of predominantly linear structure impart unique luminescent properties, electrical conductance, and biological activity to the resultant materials. Special interest is found in coordination polymers, in which the packing of the silver atoms is denser than in the metal. This feature may be conducive for the use of these polymers in electroactive composites.

Silver-containing hybrid materials already obtained hold promise for application as bactericidal substances, anti-tumor agents, and biomarkers as well as luminescent, electrically-conducting, and semiconductor systems, catalysts for chemical reactions, and sensors for chemical compounds and deformation.

REFERENCES

1. G. Kickelbick, *Progr. Polym. Sci.*, **28**, No. 1, 83-114 (2003).
2. G. Kickelbick (ed.), *Hybrid Materials. Synthesis, Characterization and Applications*, Wiley-VCH Verlag GmbH & Co., Weinheim (2007).
3. W. Knoll and R. C. Advincula (eds.), *Functional Polymer Films*, Wiley-VCH Verlag GmbH & Co., KGaA, Weinheim (2011).
4. G. L. Drisko and C. Sanchez, *Eur. J. Inorg. Chem.,* No. 32, 5097-5105 (2012).
5. J. Aleman, A. V. Chadwick, J. He, et al., *Pure Appl. Chem.*, **79**, No. 10, 1801-1829 (2007).
6. A. Yu. Olenin and G. V. Lisichkin, *Usp. Khim.*, **80**, No. 7, 635-662 (2011).
7. B. A. Rozenberg and R. Tenne, *Progr. Polym. Sci.*, **33**, No. 1, 40-112 (2008).
8. M. Karg, *Colloid. Polym. Sci.*, **290**, No. 8, 673-688 (2012).
9. E. Katz and I. Willner, *Angew. Chem. Int. Ed.*, **43**, No. 45, 6042-6108 (2004).
10. K. E. Sapsford, W. R. Algar, L. Berti, et al., *Chem. Rev.*, **113**, No. 3, 1904-2074 (2013).
11. A. A. Shemetov, I. Nabiev, and A. Sukhanova, *ACS Nano*, **6**, No. 6, 4585-4602 (2012).
12. A. D. Pomogailo, *Colloid J.*, **67**, No. 6, 658-677 (2005).
13. W. Yuan, J. Ji, J. Fu, and J. Shen, *J. Biomed. Mater Res. B*, **85**, No. 2, 556-563 (2008).
14. R. Bryaskova, D. Pencheva, G. M. Kale, et al., *J. Colloid Interface Sci.*, **349**, No. 1, 77-85 (2010).
15. P. J. Rivero, A. Urrutia, J. Goicoechea, et al., *Nanoscale Res. Lett.*, **6**, No. 1, 305 (2011).
16. X. Shao, S.-R. Zhai, B. Zhai, and Q.-D. An, *J. Sol-Gel Sci. Technol.*, **66**, No. 2, 264-273 (2013).
17. H. Wang, K.-F. Yang, L. Li, et al., *ChemCatChem*, **6**, No. 2, 580-591 (2014).
18. C. Gao, C. D. Vo, Y. Z. Jin, et al., *Macromolecules*, **38**, No. 21, 8634-8648 (2005).
19. R. Bryaskova, N. Georgieva, D. Pencheva, et al., *Colloids Surfaces A*, **444**, No. 1, 114-119 (2014).
20. V. Singh and S. Ahmad, *Cellulose*, **19**, No. 5, 1759-1769 (2012).
21. M. Malenovska, M.-A. Neouze, U. Schubert, et al., *Dalton Trans.*, **34**, 4647-4651 (2008).
22. M. Veerapandian and K. Yun, *Polym. Compos.*, **31**, No. 9, 1620-1627 (2010).
23. M. Aflori, B. Simionescu, I.-E. Bordianu, et al., *Mater. Sci. Eng. B*, **178**, No. 19, 1339-1346 (2013).
24. I. Azócar, E. Vargas, N. Duran, et al., *Mater. Chem. Phys.*, **137**, No. 1, 396-403 (2012).
25. A. C. Patel, S. Li, C. Wang, et al., *Chem. Mater.*, **19**, No. 6, 1231-1238 (2007).
26. A. Manivel, R. Sivakumar, S. Anandan, and M. Ashokkumar, *Electrocatalysis*, **3**, No. 1, 22-29 (2012).
27. A. Manivel and S. Anandan, *J. Solid State Electrochem.*, **15**, No. 1, 153-160 (2011).
28. S. K. Medda, M. Mitra, and G. De, *J. Chem. Sci.*, **120**, No. 6, 565-572 (2008).
29. B. Oktay and N. Kayaman-Apohan, *Adv. Polym. Technol.*, **32**, 21341 (2013).
30. B. Oktay and N. Kayaman-Apohan, *J. Coat. Technol. Res.*, **10**, No. 6, 785-798 (2013).

31. A. Chibac, V. Melinte, T. Buruiana, et al., *Chem. Eng. J.*, **200-202**, 577-588 (2012).
32. S. Guo, S. Dong, and E. Wang, *Chem. Eur. J.*, **15**, 2416-2424 (2009).
33. R. D. Toker, N. Kayaman-Apohan, and M. V. Kahraman, *Progr. Org. Coat.*, **76**, No. 9, 1243-1250 (2013).
34. L. Chang, Y. Ding, and X. Li, *Biosens. Bioelectron.*, **50**, 106-110 (2013).
35. E. M. Benetti, X. F. Sui, S. Zapotoczny, and G. J. Vansco, *Adv. Funct. Mater.*, **20**, 939-944 (2010).
36. F. Costantini, E. M. Benetti, R. M. Tiggelaar, et al., *Chem. Eur. J.*, **16**, 12406-12411 (2010).
37. R. Hu, G. Li, Y. Jiang, et al., *Langmuir*, **29**, No. 11, 3773-3779 (2013).
38. S. Kumar, S. P. Pawar, K. Chatterjee, and S. Bose, *Mater. Technol. B*, **1**, No. 1, 59-63 (2014).
39. H. Ozawa, N. Ide, T. Fujigaya, et al., *Chem. Eur. J.*, **17**, No. 48, 13438-13444 (2011).
40. H.-W. Tien, Y.-L. Huang, S.-Y. Yang, et al., *Carbon*, **49**, No. 5, 1550-1560 (2011).
41. Z. Xu, H. Gao, and H. Guoxin, *Carbon*, **49**, No. 14, 4731-4738 (2011).
42. R.-X. Dong, C.-T. Liu, K.-C. Huang, et al., *ACS Appl. Mater. Interfaces*, **4**, 1449-1455 (2012).
43. S. Guo, S. Dong, and E. Wang, *Small*, **4**, No. 8, 1133-1138 (2008).
44. R. Fang, X. Ge, M. Du, et al., *Colloid Polym. Sci.*, **292**, No. 4, 985-990 (2014).
45. S. P. Dubey, A. D. Dwivedi, I.-C. Kim, et al., *Chem. Eng. J.*, **244**, 160-167 (2014).
46. V. H. Luan, H. N. Tien, T. V. Cuong, et al., *J. Mater. Chem.*, **22**, 8649-8653 (2012).
47. D. Lee, H. Lee, Y. Ahn, et al., *Nanoscale*, **5**, No. 17, 7750-7755 (2013).
48. Y. Liu, Q. Chang, and L. Huang, *J. Mater. Chem. C*, **1**, 2970-2974 (2013).
49. Y. Wang, M. Tang, X. Lin, et al., *Microchim. Acta*, **176**, Nos. 3/4, 405-410 (2012).
50. G. Moad, E. Rizzardo, and S. H. Thang, *Polymer*, **49**, 1079-1131 (2008).
51. G. Moad, E. Bicciocchi, M. Chen, et al., *ACS Symp. Series*, **1100**, No. 16, 243-258 (2012).
52. J. Liu, L. Zhang, S. Shi, et al., *Langmuir*, **26**, No. 18, 14806-14813 (2010).
53. S. Fedorchuk, T. Zheltonozhskaya, Y. Gomza, et al., *Macromol. Symp.*, **317/318**, 103-116 (2012).
54. M. Długosz, M. Bulwan, G. Kania, et al., *J. Nanopart. Res.*, **14**, 1313 (2012).
55. T. Wu, Z. Ge, and S. Liu, *Chem. Mater.*, **23**, No. 9, 2370-2380 (2011).
56. H. Wang, J. Shen, G. Cao, et al., *J. Mater. Chem. B*, **1**, No. 45, 6225-6234 (2013).
57. E. Katz and I. Willner, *Angew. Chem. Int. Ed.*, **43**, 6042-6108 (2004).
58. R. Konwarh, M. Shai, T. Medhi, et al., *Ultrason. Sonochem.*, **21**, 634-642 (2014).
59. R. Contreras-Cáceres, I. Pastoriza-Santos, R. A. Álvarez-Puebla, et al., *Chem. Eur. J.*, **16**, 9462-9467 (2010).
60. R. Contreras-Cáceres, S. Abalde-Cela, P. Guardia-Girós, et al., *Langmuir*, **27**, No. 8, 4520-4525 (2011).
61. E. I. Alarcon, C. J. Bueno-Alejo, C. W. Noel, et al., *J. Nanopart. Res.*, **15**, 1374 (2013).
62. C. Aymonier, U. Schlotterbeck, L. Antonietti, et al., *Chem. Commun.*, **24**, 3018-3019 (2002).
63. M. Chen, Y. Zhao, W. Yang, and M. Yin, *Langmuir*, **29**, No. 51, 16018-16024 (2013).
64. I. Willner and E. Katz (eds.), *Bioelectronics*, Wiley-VCH GmbH & Co., KGaA, Weinheim (2005).
65. K. E. Sapsford, W. R. Algar, L. Berti, et al., *Chem. Rev.*, **113**, No. 3, 1904-2074 (2013).
66. K. Saha, A. Bajaj, B. Duncan, and V. M. Rotello, *Small*, **7**, No. 14, 1903-1918 (2011).
67. M. J. Sailor and J.-H. Park, *Adv. Mater.*, **24**, No. 28, 3779-3802 (2012).
68. S. Liu, J. Li, and Z.-Y. Li, *Adv. Opt. Mater.*, **1**, 227-231 (2013).
69. R. Martínez-Máñez, F. Sancenón, M. Hecht, et al., *Anal. Bioanal. Chem.*, **399**, 55-74 (2011).
70. K. Matsumoto, R. Tsuji, Y. Yonemushi, and T. Yoshida, *J. Nanopart. Res.*, **6**, 649-659 (2004).
71. M. Melikhov, K. Yusenko, D. Esken, et al., *Eur. J. Inorg. Chem.*, No. 24, 3701-3714 (2010).
72. J. R. Morones and W. Frey, *J. Nanopart. Res.*, **12**, 1401-1414 (2010).
73. D. F. Moyano and V. M. Rotello, *Langmuir*, **27**, No. 17, 10376-10385 (2011).
74. J. Perez-Prieto, *Photochem. Photobiol.*, **89**, 1291-1298 (2013).
75. A. Singh, S. Hede, and M. Sastry, *Small*, **3**, No. 3, 466-473 (2007).
76. Y. Song, Z. Li, L. Wang, et al., *Microsc. Res. Techniq.*, **71**, No. 6, 409-412 (2008).
77. H. Weickmann, J. C. Tiller, R. Thomann, and R. Mulhaupt, *Macromol. Mater. Eng.*, **290**, No. 9, 875-883 (2005).
78. I. Willner, B. Basnar, and B. Willner, *FEBS J.*, **274**, No. 2, 302-309 (2007).
79. N. Yufa, S. Fronk, S. B. Darling, et al., *Soft Matter*, **5**, No. 8, 1683-1686 (2009).

80. S. A. Zav'yalov, J. Schoonman, A. N. Pivkina, and R. V. Gainutdinov, *Russ. J. Phys. Chem. B*, **1**, No. 2, 171-177 (2007).
81. A. A. Zezin, V. I. Feldman, S. S. Abramchuk, et al., *Polym. Sci. C*, **53**, No. 1, 61-67 (2011).
82. J.-T. Zhang, G. Wei, T. F. Keller, et al., *Macromol. Mater. Eng.*, **295**, No. 11, 1049-1057 (2010).
83. H. El-Sherif, M. El-Masry, and A. Kansoh, *Macromol. Res.*, **19**, No. 11, 1157-1165 (2011).
84. Y. Lu, Y. Mei, M. Ballauff, and M. Drechsler, *J. Phys. Chem. B*, **110**, 3930-3937 (2006).
85. A. Pich, A. Karak, Y. Lu, et al., *Macromol. Rapid Commun.*, **27**, No. 5, 344-350 (2006).
86. J. Zhang, S. Xu, and E. Kumacheva, *J. Am. Chem. Soc.*, **126**, No. 25, 7908-7914 (2004).
87. Y. Sun, Y. Liu, G. Zhao, et al., *J. Mater. Sci.*, **43**, No. 13, 4625-4630 (2008).
88. S. U. Rehman, S. M. Shah, and M. Siddiq, *J. Chem. Soc. Pakistan*, **35**, No. 3, 717-725 (2013).
89. X. Liu, C. Zhang, J. Yang, et al., *RSC Adv.*, **3**, No. 10, 3384-3390 (2013).
90. M. Ajmal, Z. H. Farooqi, and M. Siddiq, *Korean J. Chem. Eng.*, **30**, No. 11, 2030-2036 (2013).
91. L. Koponen, L. O. Tunturivuori, M. J. Puska, and Y. Hancock, *J. Chem. Phys.*, **132**, 214301 (2010).
92. N. Zhang, X. Yu, and J. Hu, *RSC Adv.*, **3**, No. 33, 13740-13747 (2013).
93. T. Tamai, M. Watanabe, T. Teramura, et al., *Macromol. Symp.*, **282**, No. 1, 199-204 (2009).
94. T. Tamai, M. Watanabe, T. Teramura, et al., *Macromol. Symp.*, **288**, No. 1, 104-110 (2010).
95. S. Bokern, J. Getze, S. Agarwal, and A. Greiner, *Polymer*, **52**, No. 4, 912-920 (2011).
96. E. Antoniou, P. Voudouris, A. Larsen, et al., *J. Phys. Chem. C*, **116**, No. 6, 3888-3896 (2012).
97. E. Vasile, E. Rusen, A. Mocanu, et al., *Colloid Polym. Sci.*, **290**, No. 3, 193-201 (2012).
98. A. Meristoudi, S. Pispas, and N. Vainos, *J. Polym. Sci. B*, **46**, 1515-1524 (2008).
99. T. Pietsch, N. Gindy, B. Mahltig, and A. Fahmi, *J. Polym. Sci. B*, **48**, No. 14, 1642-1650 (2010).
100. J. Zhao, X. Xie, and X. Zhou, *Iran. Polym. J.*, **20**, No. 10, 845-852 (2011).
101. Y.-N. Zhou, H. Cheng, and Z.-H. Luo, *AIChE J.*, **59**, No. 12, 4780-4793 (2013).
102. D. R. Lide (ed.), *Handbook of Chemistry and Physics*, CRC Press, Boca Raton (2001).
103. X. Meng, K. Fujita, Y. Zong, et al., *Appl. Phys. Lett.*, **92**, 201112 (2008).
104. J. Chiefari, Y. K. Chong, F. Ercole, et al., *Macromolecules*, **31**, No. 16, 5559-5562 (1998).
105. W. Xu, Y. Zhu, X. Chen, et al., *Nano Res.*, **6**, No. 11, 795-807 (2013).
106. D. Dasgupta, I. K. Shishmanova, A. Ruiz-Carretero, et al., *J. Am. Chem. Soc.*, **135**, No. 30, 10922-10925 (2013).
107. M. W. Lee, M. S. Kim, and K. Kim, *J. Mol. Struct.*, **415**, Nos. 1/2, 93-100 (1997).
108. H. S. Han, C. H. Kim, and K. Kim, *Appl. Spectroscopy*, **52**, No. 8, 1047-1052 (1998).
109. D. S. Kilin, O. V. Prezhdo, and Y. Xia, *Chem. Phys. Lett.*, **458**, Nos. 1-3, 113-116 (2008).
110. T. I. Izaak, O. V. Babkina, A. I. Boronin, et al., *Colloid J.*, **65**, 720-725 (2003).
111. D. Pencheva, R. Bryaskova, and T. Kantardjiev, *Mater. Sci. Eng. C*, **32**, No. 7, 2048-2051 (2012).
112. J. Sundaram, B. Park, and Y. Kwon, *J. Nanosci. Nanotechnol.*, **13**, No. 8, 5382-5390 (2013).
113. H. Y. Son, J. H. Ryu, H. Lee, and Y. S. Nam, *ACS Appl. Mater. Interfaces*, **5**, No. 13, 6381-6390 (2013).
114. M. Rahman (ed.), *Nanomaterials*, InTech, Rijeka (2011).
115. Y. Yagci, *J. Coat. Technol. Res.*, **9**, No. 2, 125-134 (2012).
116. G. Suriati, M. Mariatti, and A. Azizan, *Polym. Bull.*, **70**, No. 1, 311-323 (2013).
117. D. Crespy and K. Landfester, *Polymer*, **50**, 1616-1620 (2009).
118. S. Kudoh and T. Orii, *Bull. Chem. Soc. Jpn.*, **86**, No. 3, 390-392 (2013).
119. M. A. Mahmoud, A. J. Poncheri, and M. A. El-Sayed, *J. Phys. Chem. C*, **116**, No. 24, 13336-13342 (2012).
120. V. Melinte, T. Buruiana, I. D. Moraru, and E. C. Buruiana, *Dig. J. Nanomater. Bios.*, **6**, No. 1, 213-223 (2011).
121. D. S. Zhang, X. Y. Liu, J. L. Li, et al., *Langmuir*, **29**, No. 36, 11498-11505 (2013).
122. M. Gladitz, S. Reinemann, and H.-J. Radusch, *Macromol. Mater. Eng.*, **294**, 178-189 (2009).
123. L. P. Balogh, S. M. Redmond, P. Balogh, et al., *Macromol. Biosci.*, **7**, 1032-1046 (2007).
124. J. A. Orlicki, N. E. Zander, G. R. Martin, et al., *J. Appl. Polym. Sci.*, **128**, No. 6, 4181-4188 (2013).
125. D. Zhang, G. Zhang, L. Chen, et al., *J. Appl. Polym. Sci.*, **130**, No. 5, 3778-3784 (2013).
126. L.-Z. Zhu, W.-B. Zhou, and J. Ji, *J. Nanopart. Res.*, **12**, No. 6, 2179-2187 (2010).
127. L. M. Davis, D. S. Thompson, C. J. Dean, et al., *J. Appl. Polym. Sci.*, **103**, 2409-2418 (2007).

128. D. Yorifuji and S. Ando, *Macromol. Chem. Phys.*, **211**, No. 19, 2118-2124 (2010).
129. Y. B. Wankhede, S. B. Kondawar, S. R. Thakare, and P. S. More, *Adv. Mat. Lett.*, **4**, No. 1, 89-93 (2013).
130. M. R. Karim, J. H. Yeum, M.-Y. Lee, et al., *Polym. Adv. Technol.*, **20**, 639-644 (2009).
131. P. Gómez-Romero and C. Sanchez (eds.), *Functional Hybrid Materials*, Wiley-VCH Verlag GmbH & Co. KGaA, Weinheim (2004).
132. D. Munoz-Rojas, J. Oro-Sole, O. Ayyadac, and P. Gomez-Romero, *J. Mater. Chem.,* **21**, 2078-2086 (2011).
133. X.-G. Li, H. Feng, and M.-R. Huang, *Chem. Eur. J.*, **16**, 10113-10123 (2010).
134. P. Routh, P. Mukherjee, and A. K. Nandi, *Langmuir*, **26**, No. 7, 5093-5100 (2010).
135. F. Tassinari, E. Tancini, M. Innocenti, et al., *Langmuir*, **28**, No. 44, 15505-15512 (2012).
136. M. Mumtaz, B. Ouvrard, L. Maillaud, et al., *Eur. J. Inorg. Chem.*, 5360-5370 (2012).
137. B. V. K. Naidu, J. S. Park, S. C. Kim, et al., *Solar Energy Mater. Solar Cells*, **92**, 397-401 (2008).
138. K.-Y. Chun, Y. Oh, J. Rho, et al., *Nature Nanotechnol.*, **5**, 853-857 (2010).
139. K. Immonen, K. Nattinen, J. Sarlin, and J. Hartikainen, *J. Appl. Polym. Sci.*, **114**, No. 3, 1494-1502 (2009).
140. H. Weickmann, J. C. Tiller, R. Thomann, and R. Mulhaupt, *Macromol. Mater. Eng.*, **290**, No. 9, 875-883 (2005).
141. F. Fang, W. Yang, and S. Yu, *Appl. Phys. Lett.*, **104**, 132909 (2014).
142. A. O. Govorov, G. W. Bryant, W. Zhang, et al., *Nano Lett.*, **6**, No. 5, 984-994 (2006).
143. A. L. Tolstov, *Teor. Éksp. Khim.*, **49**, No. 6, 331-353 (2013). [*Theor. Exp. Chem.*, **49**, No. 6, 347-370 (2014) (English translation).]
144. D. Ma, X. Xie, and L.-M. Zhang, *J. Polym. Sci. B*, **47**, 740-749 (2009).
145. C. Schmidtke, H. Kloust, N. G. Baustus, et al., *Nanoscale*, **5**, No. 23, 11783-11794 (2013).
146. J. George, V. A. Sajeevkumar, K. V. Ramana, et al., *J. Mater. Chem.*, **22**, 22433-22439 (2012).
147. S. Ghosh, T. K. Ranebennur, and H. N. Vasan, *Int. J. Carbohydr. Chem.*, 693759 (2011).
148. M. S. Islam and J. H. Yeum, *Colloids Surfaces A*, **436**, 279-286 (2013).
149. W. Xiao, J. Xu, X. Liu, et al., *J. Mater. Chem. B*, **1**, No. 28, 3477-3485 (2013).
150. H. Penchev, D. Paneva, N. Manolova, and I. Rashkov, *Macromol. Biosci.*, **9**, No. 9, 884-894 (2009).
151. V. K. Rana, O. S. Kushwaha, and R. P. Singh, *Macromol. Res.*, **18**, No. 9, 845-852 (2010).
152. D. Huo, J. He, S. Yang, et al., *J. Colloid Interface Sci.*, **393**, 119-125 (2013).
153. D. R. Bagal-Kestwal, R. M. Kestwal, W.-T. Hsieh, and B. H. Chiang, *J. Pharm. Biomed. Anal.*, **88**, 571-578 (2014).
154. X. Wang, F. He, X. Zhu, et al., *Sci. Rep.*, **4**, 4406 (2014).
155. S. Taheri, G. Baier, P. Majewski, et al., *J. Mater. Chem. B*, **2**, No. 13, 1838-1845 (2014).
156. O. Ayyad, D. Munoz-Rojas, J. Oro-Sole, and P. Gomez-Romero, *J. Nanopart. Res.*, **12**, 337-345 (2010).
157. E. Muthuswamy, S. S. Ramadevi, H. N. Vasa, et al., *J. Nanopart. Res.*, **9**, 561-567 (2007).
158. R. R. Ramazanov and A. Kononov, *J. Phys. Chem. C*, **117**, No. 36, 18681-18687 (2013).
159. I. L. Volkov, R. R. Ramazanov, E. V. Ubyivovk, et al., *ChemPhysChem*, **14**, No. 15, 3543-3550 (2013).
160. C. E. Chivers, E. Crozat, C. Chu, et al., *Nature Methods*, **7**, 391-393 (2010).
161. S. Rudiuk, A. Vanancio-Marquez, G. Hallais, and D. Baigl, *Soft Matter.*, **9**, 9146-9152 (2013).
162. A. Dawn and A. K. Nandi, *J. Phys. Chem. B*, **110**, No. 37, 18291-18298 (2006).
163. J. Li, Q. He, and X. Yan (eds.), *Molecular Assembly of Biomimetic Systems*, Wiley-VCH Verlag GmbH &Co., KGaA, Weinheim (2011).
164. J. J. Martin, J. M. Cardamone, P. L. Irwin, and E. M. Brown, *Colloids Surfaces B*, **88**, 354-361 (2011).
165. G. E. Adamov, K. S. Levchenko, V. R. Kurbangaleev, et al., *Russ J. Gen. Chem.*, **83**, No. 11, 2195-2202 (2013).
166. G. E. Adamov, E. V. Zinov'ev, P. S. Shmelin, et al., *Nanoinzheneriya,* **12**, 13-20 (2013).
167. G. E. Adamov, I. S. Goldobin, E. P. Grebennikov, and A. G. Devyatkov, *Khim. Vysok. Energ.*, **42**, No. 4, 21-22 (2008).
168. Y. Liu, X. Liu, X. Wang, et al., *J. Appl. Polym. Sci.*, **116**, No. 5, 2617-2625 (2010).
169. M. E. Alf, A. Asatekin, M. C. Barr, et al., *Adv. Mater.*, **22**, No. 18, 1993-2027 (2010).
170. V. Apalangya, V. Rangari, B. Tiimob, et al., *Appl. Surf. Sci.*, **295**, 108-114 (2014).
171. P. Graf, A. Mantion, A. Foelske, et al., *Chem. Eur. J.*, **15**, 5831-5844 (2009).
172. G. Maayan and L.-K. Liu, *Peptide Sci.*, **96**, No. 5, 679-687 (2011).
173. V. Bonačić-Koutecký, A. Kulesza, L. Gell, et al., *Phys. Chem. Chem. Phys.*, **14**, No. 26, 9282-9290 (2012).

174. Ž. Sanader, R. Mitrić, V. Bonačić-Koutecký, et al., *Phys. Chem. Chem. Phys.*, **16**, No. 3, 1257-1261 (2014).
175. Q. Dong, H. Su, W. Cao, et al., *Mater. Chem. Phys.*, **110**, 160-165 (2008).
176. L. T. Yu, I. A. Banerjee, and H. Matsui, *J. Am. Chem. Soc.*, **125**, No. 48, 14837-14840 (2003).
177. O. Carny, D. E. Shalev, and E. Gazit, *Nano Lett.*, **6**, No. 8, 1594-1597 (2006).
178. A. Abbas, R. Kattumenu, L. Tian, et al., *J. Nanosci. Lett.*, **2**, No. 10, 1-16 (2012).
179. S.-Y. Lee, J.-S. Lim, and M. T. Harris, *Biotechnol. Bioeng.*, **109**, No. 1, 16-30 (2012).
180. G. Plascencia-Villa, J. M. Saniger, J. A. Ascencio, et al., *Biotechnol. Bioeng.*, **104**, No. 5, 871-881 (2009).
181. E. Dujardin, C. Peet, and G. Stubbs, *Nano Lett.*, **3**, No. 3, 413-417 (2003).
182. A. N. Khlobystov, A. J. Blake, N. R. Champness, et al., *Coord. Chem. Rev.*, **222**, No. 1, 155-192 (2001).
183. S. Hamamci, V. T. Yilmaz, and W. T. A. Harrison, *Struct. Chem.*, **16**, No. 4, 379-383 (2005).
184. A. G. Young and L. R. Hanton, *Coord. Chem. Rev.*, **252**, Nos. 12/14, 1346-1386 (2008).
185. D. R. Witcomb and M. Rajeswaran, *J. Coord. Chem.*, **59**, No. 11, 1253-1260 (2006).
186. R. J. T. Houk, B. W. Jacobs, F. El Gabaly, et al., *Nano Lett.*, **9**, No. 10, 3413-3418 (2009).
187. M. P. Suh, H. R. Moon, E. Y. Lee, and S. Y. Jang, *J. Am. Chem. Soc.*, **128**, No. 14, 4710-4718 (2006).
188. H. R. Moon, J. H. Kim, and M. P. Suh, *Angew. Chem. Int. Ed.*, **44**, No. 8, 1261-1265 (2005).
189. W.-Y. Bi, W.-L. Chai, X.-Q. Lu, et al., *J. Coord. Chem.*, **62**, No. 12, 1928-1938 (2009).
190. A. Bondi, *J. Phys. Chem.*, **68**, No. 3, 441-451 (1964).
191. F. F. Li, J. F. Ma, S. Y. Song, et al., *Inorg. Chem.*, **44**, No. 25, 9374-9383 (2005).
192. A. Earnshaw and N. Greenwood (eds.), *Chemistry of the Elements*, Pergamon Press, Oxford (1984).
193. E. Bosch and C. L. Barnes, *J. Coord. Chem.*, **58**, No. 12, 1021-1027 (2005).
194. S. E.-D. H. Etaiw, M. M. El-Bendary, et al., *J. Coord. Chem.*, **63**, No. 6, 1038-1051 (2010).
195. C. N. R. Rao, A. Ranganathan, V. R. Pedireddi, and A. R. Raju, *Chem. Commun.*, No. 1, 39-40 (2000).
196. I. Kalf, M. Braun, Y. Wang, and U. Englert, *Cryst. Eng. Commun.*, **8**, No. 12, 916-922 (2006).
197. Y. Wei, Y. Song, H. Hou, et al., *J. Coord. Chem.*, **57**, No. 15, 1329-1337 (2004).
198. X.-Y. Liu and H.-L. Zhu, *Synth. React. Inorg. Metal-Org. Nano-Metal Chem.*, **35**, No. 2, 155-159 (2005).
199. A. A. Mohammed, *Coord. Chem. Rev.*, **254**, Nos. 17/18, 1918-1947 (2010).
200. A. Tabacaru, C. Pettinari, F. Marchetti, et al., *Inorg. Chem.*, **51**, No. 18, 9775-9788 (2012).
201. P. J. Steel and C. M. Fitchett, *Coord. Chem. Rev.*, **252**, Nos. 8/9, 990-1006 (2008).
202. J.-H. Yang, S.-L. Zheng, X.-L. Yu, and X.-M. Chen, *Cryst. Growth Des.*, **4**, No. 4, 831-836 (2004).
203. X.-Y. Liu and H.-L. Zhu, *Synth. React. Inorg. Metal-Org. Nano-Metal Chem.*, **35**, No. 4, 325-332 (2005).
204. T. V. Slenters, J. L. Sagué, P. S. Brunetto, et al., *Materials*, **3**, No. 5, 3407-3429 (2010).
205. E. Senel, V. T. Yilmaz, and W. T. A. Harrison, *Z. Naturforsch. B*, **60**, No. 6, 659-662 (2005).
206. L. Xie, A. Ning, and X. Li, *J. Coord. Chem.*, **62**, No. 10, 1604-1612 (2009).
207. S.-L. Zheng, M.-L. Tong, H.-L. Zhu, et al., *J. Chem. Soc., Dalton Trans.*, No. 13, 2049-2053 (2001).
208. X. Yin, M.-B. Xie, W.-G. Zhang, and J. Fan, *Acta Crystallogr. E*, **63**, No. 9, 2273 (2007).
209. O. Z. Yesilel, G. Kastas, C. Darcan, et al., *Inorg. Chim. Acta*, **363**, No. 8, 1849-1858 (2010).
210. D. Sun, R. Cao, J. Weng, et al., *J. Chem. Soc., Dalton Trans.*, No. 3, 291-292 (2002).
211. R. Wang, M. C. Hong, J. Luo, et al., *Inorg. Chim. Acta*, **357**, No. 1, 103-114 (2004).
212. J.-Y. Wang, L.-Z. Zhang, W. Gu, et al., *J. Coord. Chem.*, **59**, No. 15, 1685-1691 (2006).
213. J. Wu and J.-Q. Liu, *Synth. React. Inorg. Metal-Org. Nano-Metal Chem.*, **40**, No. 1, 27-31 (2010).
214. N. Vilvamani, T. Gupta, R. D. Gupta, and S. K. Aswathi, *RSC Adv.*, **4**, No. 38, 20024-20030 (2014).
215. M. Mitsuishi, H. Tanaka, M. Obata, and T. Miyashita, *Langmuir*, **26**, No. 19, 15117-15120 (2010).
216. P. V. Kamat, *J. Phys. Chem. B*, **106**, No. 32, 7729-7744 (2002).
217. M. Rycenga, C. M. Cobley, J. Zeng, et al., *Chem. Rev.*, **111**, No. 6, 3669-3712 (2011).
218. S. Zhang, X. Yang, Y. Numata, and L. Han, *Energy Environ. Sci.*, **6**, No. 5, 1443-1464 (2013).
219. A. Jena, S. P. Mohanty, and P. Kumar, *Trans. Indian Ceram. Soc.*, **71**, No. 1, 1-16 (2012).